IEEE Access
Multidisciplinary | Rapid Review | Open Access Journal

Received January 13, 2022, accepted February 4, 2022, date of publication February 10, 2022, date of current version February 18, 2022.

Digital Object Identifier 10.1109/ACCESS.2022.3150905

Transverse Flux Machine–A Review

BENEDIKT KAISER AND NEJILA PARSPOUR
Institute of Electrical Energy Conversion, University of Stuttgart, 70569 Stuttgart, Germany
Corresponding author: Benedikt Kaiser (benedikt.kaiser@iew.uni-stuttgart.de)

This work was supported by the Deutsche Forschungsgemeinschaft (DFG) as part of the International Research Training Group "Soft Tissue Robotics" (GRK 2198/1).

ABSTRACT For applications with high torque demand, gearboxes are commonly used to convert torque and speed in order to receive higher specific values for torque and power. This causes additional losses, cost, inaccuracies, effort, and noise. Eliminating the need of a mechanical gear and the associated disadvantages, Transverse Flux Machines with their high torque density are a very promising alternative. Despite a high torque density and a high efficiency, these types of machines are not commonly used. Due to the complex structure, challenges with mechanical design, and modeling of the machine behavior arise. Additionally, there are high requirements for the inverter due to the low power factor. This paper provides an overview of the state of the art including the potentials and advantages but also the problems and hindrances of these types of machines. Relating to linear and rotary machines from research and industry, the machine is introduced with its history, application and classification. Further, the general technical aspects, the influence of materials for flux guidance, the methods of modeling, methods for a minimization of torque ripples, as well as methods for power factor improvement are presented.

INDEX TERMS Direct drive, electric machines, modulated pole machines, permanent magnet machines, power factor, review, rotating machines, torque density, torque ripple, transverse flux machines.

I. INTRODUCTION

This review aims to paint a complete picture of the Transverse Flux Machine (TFM) considering all significant international references.

The main characteristics are the comparably high gravimetric torque density and the high efficiency, providing ideal preconditions for application as direct drive without the need of a gearbox [1]. Hence, disadvantages of gearing with elastics, backlash, and noise are eliminated. Drawbacks are typically high torque ripples, complex design, nonlinear dynamics, and low power factor [1].

A. HISTORY

The concept of the Transverse Flux Machine was introduced by W. M. Mordey in 1890 as electric generator [2]. In 1937, a transverse flux technology for a suspension railway was presented which was not used for propulsion, but to overcome the force of gravity [3]. The transverse flux principle was reintroduced in 1971 by E. R. Laithwaite and J. F. Eastham from the Imperial College of Science Technology London [4]–[6] as linear motor. Simultaneously, first developments of the Transrapid technology with transverse magnetic circuits are presented [7]. In 1986, H. Weh from TU Braunschweig identified the capabilities of the Transverse Flux Machines with their very high achievable force density and the possible application as direct drive without the need of a gearbox [8]–[12]. Research on this machine is ongoing to date. However, large-scale industrial applications still have not been implemented.

The associate editor coordinating the review of this manuscript and approving it for publication was Paolo Giangrande.

B. APPLICATIONS

Some typical applications for these machines are connected with the term of mobility. They are considered as propulsion motor of ships [13]–[16], in aerospace applications [17]–[19], spacecraft application [20], in railway applications with rotating [21], [22] or linear [23] principle, bus applications [24], [25] with prototype TFM motor and generator in serial hybrid layout [26]–[29], as traction drive in E-Bikes [30]–[32], and in the automotive sector [33], [34]. This type of machine is considered as a traction [35]–[42] or an in-wheel traction [43]–[48] drive in electric vehicles or hybrid electric vehicles [49] as well as in peripheral applications like starter generators [35], [50].

Furthermore, TFMs are considered as electric generators in the field of renewable energy systems. They are used as direct

drive solutions in wind turbines [11], [51]–[72], wave energy generators [73]–[75] and in hydro-power plants [76]–[79].

In addition, robotic systems, such as articulated robot arms, comprise a promising scope of operation. The high torque demand and low speed of a single joint correspond with the characteristics of a TFM, investigated in [1], [80]–[84]. A linear robotic actuator is presented in [85], as well as a similar type mentioned in [86], which serves as actuator for a conveyor. In [87], [88] a linear actuator for stocker system in the display industry is illustrated. Industrial applications are presented for instance in [89] as a mechanical press and in [90] as example for the weaving and knitting industry. In [91], the utilization as direct drives in an extruder for an injection molding machine and in a turntable are examined. For industrial or automation applications, the employment as servo motor is examined in [90], [92]–[94]. The application in power tools is considered in [95].

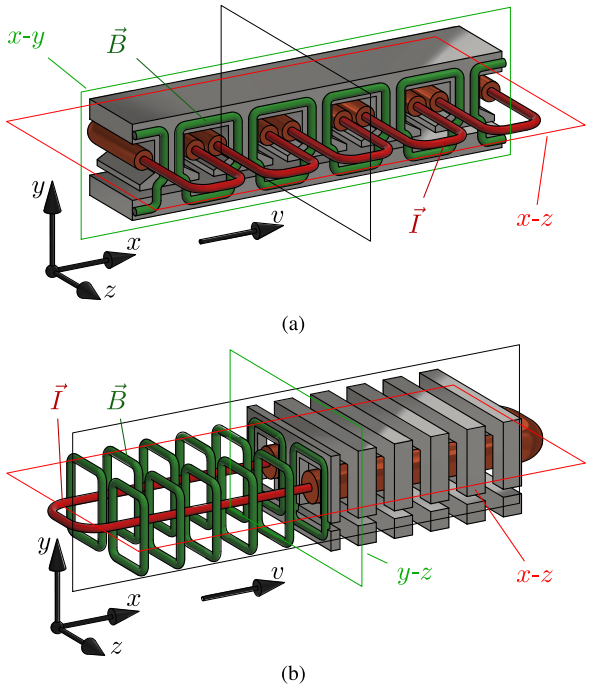

FIGURE 1. Definition of a (a) conventional and a (b) transversal flux machine in linear principle with movement in the direction of the x-axis according to [4]. Sectional view with soft-magnetics (gray), electrical conductors (copper), magnetic flux path (green), and electric current (red).

C. DEFINITION OF THE TRANSVERSE FLUX MACHINE

The term "Transverse Flux Machine" was originated by [4] and refers to the direction of the magnetic flux, which occurs mainly on a plane transverse to the moving direction. A comparison to conventional machines in linear design is illustrated in Fig. 1. For conventional machines, in Fig. 1a the plane of the magnetic flux (x-y) is in parallel with the movement in the direction of the x-axis. For the Transverse Flux Machine presented in Fig. 1b, the plane of the magnetic flux (y-z) is perpendicular to the movement. For both principles, the current corresponds with the x-z-plane.

In Fig. 2, the principles of rotating TFM, Radial Flux Machine (RFM) and Axial Flux Machine (AFM) are displayed. In order to obtain a torque, the linear principles are wrapped around an axis. For the TFM (Fig. 2a), the linear TFM arrangement is spooled around the z-axis. The RFM (Fig. 2b) and the AFM (Fig. 2c) are created by spooling the arrangement of the conventional machine (Fig. 1a) around an axis parallel to the z- or to the y-axis.

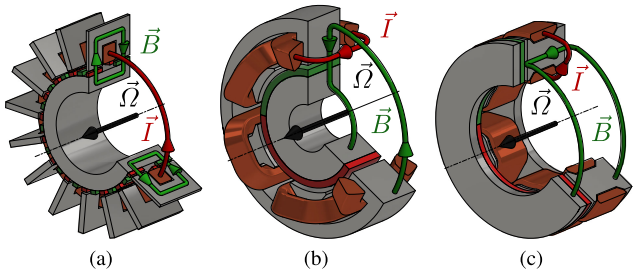

FIGURE 2. Principles of rotating (a) transverse flux machine (TFM), (b) radial flux machine (RFM), and (c) axial flux machine (AFM) with rotation axis $\vec{\Omega}$ (black), main flux $\vec{B}$ (green), and current $\vec{I}$ (red).

In publications [34], [96]–[104] the machine is named "Modulated Pole Machine" (MPM), coined by the scientists of Newcastle University, UK and Höganäs AB, Sweden. This stems from the principle of the modulation of a two-pole field from a ring-coil into multi-pole field [34], [105].

II. CLASSIFICATION

The authors [78], [106], [107] classify these types of machines via a tree-structure. Due to the expanding tree-structure resulting from of the various possibilities of the arrangement of these machines and their components, the TFMs are classified in this paper by listing specific characteristics in analogous to classification presented in [108] as a suggestion for future classification.

A. CLASSIFICATION VIA MOVEMENT

The simplest form of classification of machines is based on their movement. Typically, this is divided into linear or rotary, whereby the machines generate either a force or a torque in motor operation. Rotating machines are separated into inner-rotor and outer-rotor, depending on the arrangement of rotor and stator. Moreover, there is the possibility of a double-sided arrangement which is also valid for linear machines.

B. CLASSIFICATION VIA EXCITATION

In [1], the general concepts of TFMs regarding excitation in addition to excitation by stator-winding is divided into three categories: passive reluctance rotor machines, passive rotor machines with excitation on the stator, and machines with PMs on the rotor. The review revealed two additional categories: the electrically excited rotor machine and the induction machine.

1) PASSIVE ROTOR

The generation of torque in passive rotor machines is based on the reluctance principle. Examples of switched reluctance (SR) TFMs are given in [50], [109]–[114]. Since there is no need for PMs, reluctance machines have cost advantages and are suitable for high temperature applications [110].

2) (PERMANENT MAGNET) EXCITED STATOR WITH PASSIVE ROTOR

Within this design, all sources of magnetomotive force, current carrying coil and PMs, are located on the stator. Depending on the rotor position, the main-flux is switched clockwise or counter-clockwise around the stator-coil by a path of soft-magnetic materials with a lower reluctance [78]. This accounts for the name ''Flux Switching Machine'' [96], [115], [116] or ''Flux-Reversal Machine'' [117], [118]. Different designs are described in [119]–[122]. In [88], [123], a linear actuator is presented, in contrast to the discussed design with PMs and a coil on the mover side, the stator is iron only.

In [124]–[126], the field is optimized by a stator- and rotor-mount PM-shielding increasing the force density compared to reluctance type.

A design with an excitation by a field winding on the stator instead of PMs is presented in [127].

3) PERMANENT MAGNET EXCITED ROTOR

Typically, PM excited rotors of TFMs are built in three configurations: surface-mounted (SM), flux-concentrating (FC) and axially magnetized (AX). For SM-configurations (Fig. 3a), the PMs are mounted directly on the rotor surface, whereas the main-flux in FC-configurations (Fig. 3b) flows through pole pieces of soft-magnetic material [128]. In comparison to TFMs in SM-configuration, TFMs in FC-configuration have the potential to offer a higher torque, but are associated with higher torque ripple as well [129]–[131]. In [132], [133], a complex layout with flux-concentrating and leakage reduction magnets is outlined. Structures with AX magnets (Fig. 3c) are illustrated in [134], with cuboids between the pole pieces or with ring- or disc shape magnets for rotating machines [67], [135]–[139].

4) ELECTRICALLY EXCITED ROTOR

For the category of the electrically excited TFM, there are a few publications only [76], [140]. Usually, the rotor is excited by field coils carrying DC-Current. Reference [140] presents a Finite Element Analysis (FEA) with an electrically excited rotor, including a contactless energy transfer.

5) INDUCTION MACHINES

Machines utilizing asynchronous principles with an induced current in the rotor are identified as transverse flux linear induction motor [4], [141], [142], or as a rotational induction motor [143], [144].

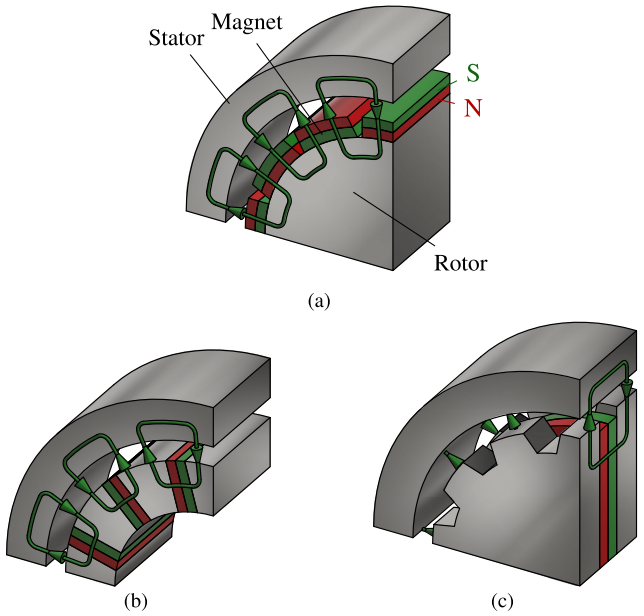

FIGURE 3. Configurations of permanent magnet excited rotors of TFMs: (a) surface-mounted (SM), (b) flux-concentrating (FC), and (c) axially magnetized (AX).

C. CLASSIFICATION VIA CORE-STRUCTURE

An additional characteristic to classify TFMs is the core structure of the stator. The most popular structures are discussed below.

1) U-CORE

A plain design of a TFM is the assembly with U-shaped cores of soft magnetic material in Fig. 4a, which are located in the distance of a double pole pitch [145]. For rotational TFMs, the U-cores are arranged circumferentially around the rotation axis. Examples for this type of machine are described in [10], [11], [38], [39], [109], [134], [146]–[149]. The in [150] presented stator uses chamfered U-cores for a better utilization of soft magnetic material, resulting in an elliptical design. Disadvantages of the concept with single U-cores are the demanding positioning in assembly [111] and the need for a carrier. As a result, typically $>50\%$ of the enclosed volume by the yoke is non-magnetic material [111]. Finally, only the magnets of every second pole pitch are used for torque generation in a specific rotor position.

The papers [10], [11], [60], [151], [152] address this disadvantage and present the double-sided stator design, which is capable to use every pole pitch for torque generation. Alternatively, in papers [67], [153]–[155], the shape of the ''U'' is changed. It widens and shears towards the air gap. The main-flux of every second pole pitch is directed around the same coil, resulting in two coils per phase (see Fig. 9).

2) U-CORE WITH I-BRIDGE

The U-core with I-brigde (UI) has an additional return path added to the U-core construction, see Fig. 4b. The advantages of this configuration consist of an increased performance and

a reduced cogging torque due to the utilization of the inactive (not contributing to the generation of torque) PMs of the U-core structure [131], [156] and the reduced stray flux due to the additional return path [145]. The shape of the I-core is often adapted in order to reduce the stray flux between the U- and I-cores. The main-flux of the rotor yoke is in tangential direction, which enables the separation of the yoke in two parts [145]. Examples for these machines are described in [10], [11], [135], [145], [157]–[159] or in [68], [156], [160] where the I-core is referred to as ''magnetic shunt''. For this design, a double-sided structure is possible [10], [11], [156].

3) C-CORE

At first glance, the C-structure in Fig. 4c resembles the U-structure . Therefore, this is not described uniformly in publications as in [69], [161], in which the U-core is referred to as C-core. The shape of the air gap is an essential feature to distinguish the C- from the U-core. For the U-core, the air gap creates a single plane (linear) or a single cylinder surface (rotating). Whereas the description of the air gap of the C-core requires at least two planes, two cylinder surfaces, or a combination of the two, depending on the position of the air gap in the flux path. Examples of this configuration are publicized in [13], [45], [59], [114], [128], [162]–[169] with various design characteristics.

4) CP-CORE

The Claw-Pole (CP) or O-core [82], [170] structure is illustrated in Fig. 4d. The direction of the main flux in the rotor is a characteristic of CP-TFMs, which is almost entirely in a plane, enabling the usage of laminations in the rotor yoke [82]. The claws cover the entirety or the majority of the width of the air gap, guiding the transverse components of the flux. There are various examples for CP-TFMs [42], [81]–[83], [92], [93], [95], [170]–[179].

The CP-TFM should not be mistaken for Claw-Pole Machines (CPMs). CPMs are known from the alternator application in automotive [180]. In contrast to the CP-TFM, the rotor and not the stator of the CPM is excited by a current in a ring winding whose field is modulated by the claw structure. The stator usually resembles that of an RFM.

5) E-CORE

In Fig. 4e an example of an E-core structure is illustrated. The air gap flux direction of the outer parts of the E-core is opposite to the direction of the flux in the middle part. The current in the two windings of E-core TFMs flows in opposite directions. This design is suitable for linear TFMs such as the machines in [88], or rotating machines with circumferential arranged phases in [46], [181]–[187]. TFMs with a single winding per core element are presented in [132], [133], [142], [188], [189]. Further, the design of the machine in [190] has an E-core built out of a C-core with an additional bridge core. It should be noted that the flux of this arrangement flows differently than the flux in the structure of Fig. 4e.

6) Z-CORE

The design with Z-core in Fig. 4f is presented in [191]. In an examination [192], additional design guidelines are expanded due to the remarkable leakage flux. In more recent research, this type is investigated with double-sided FC-PM-design [133], [193]–[196].

7) ALTERNATIVE STRUCTURES

Structures with so-called ''9''-core described in [197], [198], ''H''-core [72], and the group of tubular types [6], [199]–[209] are neither mentioned, nor further illustrated in this paper.

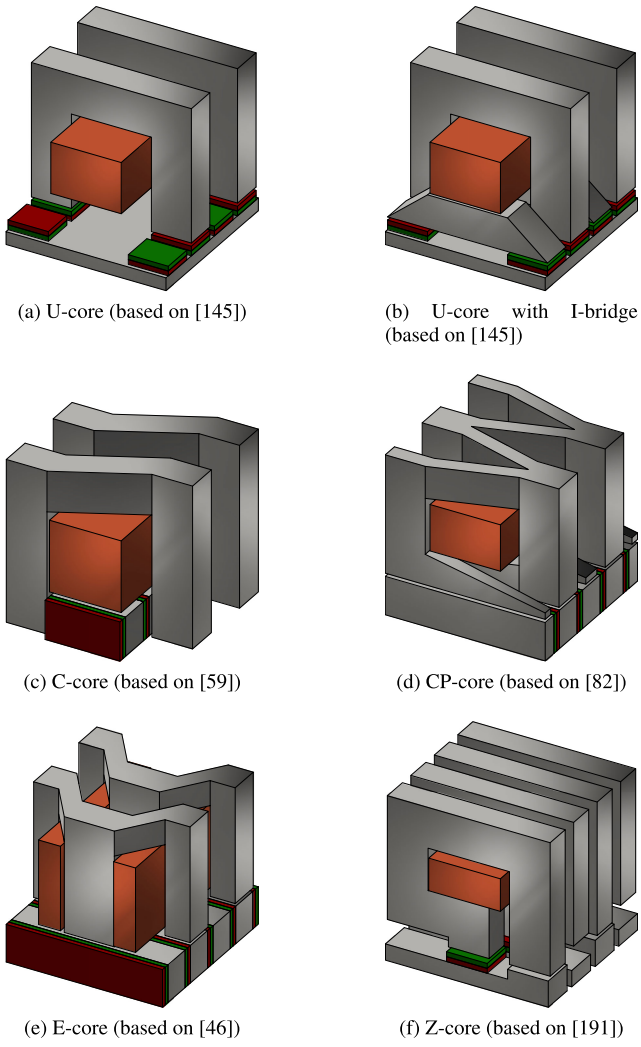

(a) U-core (based on [145])
(b) U-core with I-bridge (based on [145])
(c) C-core (based on [59])
(d) CP-core (based on [82])
(e) E-core (based on [46])
(f) Z-core (based on [191])

FIGURE 4. Overview of core structures with coil (colored in copper), magnets (green/red), and soft magnetic material (gray) of main flux path.

D. CLASSIFICATION VIA SOFT-MAGNETIC MATERIALS

The choice of soft-magnetic materials has an influence on the design and the ratings of the machines. Typical machines are separated in laminated machines, Soft-Magnetic-Composite (SMC) machines and hybrid machines. More information

about influence of soft-magnetic materials can be found in section IV.

E. CLASSIFICATION VIA ARRANGEMENT OF PHASES

Another category to structure TFMs is the spatial arrangement of phases. The axial arrangement (Fig. 5a) has the advantage of a modular design which enables the increase of torque by modularly increasing of the number of the phases [58]. Besides the axial arrangement, the phases are added up in circumferential direction (Fig. 5b) [45], [155], [169], [184], [210], [211]. This has the advantage of a flat design, accepting inactive sections for torque production between the phases and unbalanced magnetic forces, thereby causing mechanical vibrations [210]. Transferring these structures to a linear topology, the phases are arranged side by side (related to axial arrangement, Fig. 5a) or one behind the other (related to circumferential arrangement, Fig. 5b).

Additionally, there are designs in which the mechanical coupling of the phases is realized by mechanic solutions e.g. by gearing (Fig. 5c) as presented in [84], or by constructions as presented in [212] with single integrated phases in each of the two bearing blocks of a water wheel. This results in spatially distributed phases.

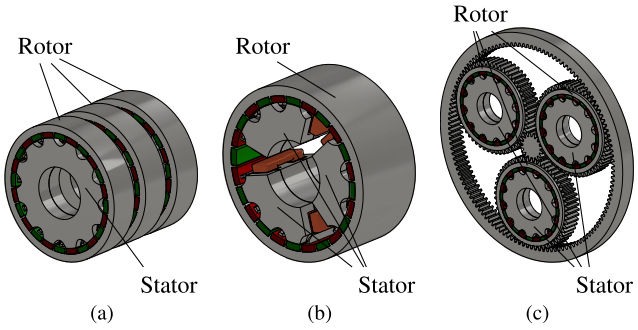

FIGURE 5. Mechanical arrangement of phases: (a) axially arranged, (b) circumferentially arranged, (c) spatially distributed, design based on structure of [81].

III. SUMMARY OF ADVANTAGES, TECHNICAL CHALLENGES AND COMPARISONS OF TFMs

As illustrated in the following, the research on TFMs is motivated by the specific advantages of the machine concept, although the broad application is inhibited by a lack of satisfactory solutions to certain challenges. This section presents the advantages and disadvantages mentioned in the examined publications. Further, a summary of comparisons with conventional machines and a comparison of prototype-TFMs is presented.

A. ADVANTAGES OF TFMs

The advantages of TFMs compared to conventional machines discussed in the reviewed publications are listed below.

1) HIGH TORQUE DENSITY

The high torque density of TFMs is the major advantage mentioned in multiple publications. In a comparison [213], [214], TFMs are able to provide a high specific tangential force compared to conventional machines (def. of Fig. 1a). This offers the potential of a direct drive solution with the elimination of the gearbox, preventing associated losses. Depending on the specific application, the TFM offers opportunities of a higher total efficiency for the electric drive train.

2) DECOUPLED MAGNETIC AND ELECTRICAL DESIGN PARAMETERS

One main advantage of the TFM-concept is the decoupling of electric and magnetic design parameters and thus the loading [8], [57], [215]. With these degrees of freedom, a large coil cross-section with convenient slot shapes is achieved [8].

Likewise, the magnetic path has less restrictions in design. A small pole pitch is possible without affecting the coil cross-section [8], thus enabling the high torque density.

3) MISSING END WINDINGS

Due to the ring-coil of the stator windings, the conductor length is minimized and reduced to the circumferential dimension [8]. Compared to a RFM, there are no end windings, which is beneficial for the resistive loss and reducing the copper mass [153]. Additionally, a higher winding slot fill-factor is achieved [111].

4) INDEPENDENT PHASES

The mechanical independence of the phases leads to an easier scaling of the number of phases. Neglecting the magnetic coupling between the phases (which is not as strong as in RFMs) enables a fast preliminary design process. Besides benefits in production [215] this results in advantages, such as the power-scaling of the machines and the exploitation of installation space due to spatially distributed phases.

In [58], the power-scaling by the number of phases is presented. Especially the lower cost of a phase-modular design with a single converter per module is pointed out. Cost-reducing scale effects are predicted particularly for a design with SMC off-tool parts.

A further advantage of mechanical independent phases is the possibility to implement a flat design of a TFM. Flat arrangements are challenging for conventional machines [216]. Therefore, designs adapted to the construction space is considered such as the circumferential (Fig. 5b) or distributed (Fig. 5c) arrangement of phases described in section II.

In order to avoid problems at startup, at least two phases with an electrical angle of $\pi/2$ should be used to generate torque in every position of the shaft and to fix the direction of movement [128], [217].

5) FAULT TOLERANCE

With the double-sided stator design and the two windings of the machine it is possible to improve the fault tolerance [194] with an appropriate power electronics and control. This also applies to a machine with multiple segments per phase with appropriate design of the coils. Further, due to the spatially separated phases it is expected to reduce the risk of a short-circuit between the phases compared to RFM with distributed windings.

6) THERMAL

The concept of a TFM is beneficial in terms of thermal properties. Because of the more tightly wound tangential coils the higher surface contact improves thermal heat conductivity [95]. The stator teeth act as cooling vanes, enabling an advantageous air cooling [18].

B. TECHNICAL CHALLENGES

Besides the above mentioned advantages of these machines, unsatisfactory solutions for technical challenges still hinder the broad application.

1) THREE-DIMENSIONAL FLUX PATH

Due to the asymmetry of the flux in 3D (so-called 3D flux path), these machines have a complex structure. Consequently, manufacturing and assembly of TFMs is often elaborate and cost-intensive [18], [215]. There are different approaches to arrange the soft magnetic components for flux guidance to achieve a high torque density. Further details can be found in section IV.

2) POLE PITCH

Typically, these machines have a high number of pole pairs with a small mechanical pole pitch. Hence, angular misalignments have a strong effect [218], which is a problem especially for small machines [83]. Besides increasing costs due to the demanding manufacturing tolerances, limitations in position sensor capability are critical [47]. Even small errors in measurement of the rotor angle influence the control behavior of the machine in a negative way [35]. Additionally, for a comparatively low speed there has to be a corresponding high frequency of the current resulting in higher hysteresis losses, eddy current losses, AC-copper losses, and inverter losses. AC-effects should be considered for precise calculations of TFMs [219].

3) MODELING AND SIMULATION

Due to the three-dimensional flux path, the flux distribution characteristic has to be solved for a three-dimensional geometry. With the longer calculation time compared to problems of a two-dimensional geometry, the optimization process with its typically high number of iterations is time-intensive. In addition, the analytical modeling of dynamics is challenging. Possible solutions are presented in section V.

4) NOISE AND TORQUE RIPPLES

Due to the principle of function of TFMs, there is a large derivation of the magnetic reluctance during one period of movement. Hence, these machines have high cogging torque as well as large torque ripple. Further, unbalanced magnetic forces induce vibrations and cause noise [60], [146], [220] or lead to destruction because of structural resonances [221]. There are several solutions to reduce these torque ripples, either by control or by mechanical design, discussed in section VI.

5) LOW POWER FACTOR

One major disadvantage of the TFM compared to conventional RFM is the low power factor, causing the need for highly overrated power converters [18], [154], [222]. Further details are discussed in section VII.

6) MAGNETIC INSULATION BETWEEN THE PHASES

In order to obtain a magnetic decoupling, there has to be a magnetic insulation between the single phases. Regularly, this is implemented by an additional air gap in axial direction. The gap has to be notably larger than the air gap between rotor and stator [98], causing lower installation space utilization. A possible solution is addressed in section IV. Experiments have shown that the often presumed magnetic independence of phases is conceivably not correct [223].

C. COMPARISON OF TFM WITH RFM AND AFM

In the following, a selection of papers is summarized. The subject of these papers is the comparison of the TFM with RFM and AFM principles. Due to the focus on specific applications with different conditions, the papers are regarded individually.

1) SWITCHED RELUCTANCE MACHINES [111]

In [111], a SR-TFM and a SR-RFM are compared. The RFM has a 12-8 configuration, the same outer (150mm) and bore (90.5mm) diameter and a length of 210mm (TFM: 185mm). Comparing the torque capability, the SR-TFM has a 50% higher torque with only 67% of copper volume. A negative influence on torque generation is the increased inductance of SR-TFM, which reduces the slope of the current.

2) SERVO DRIVE [171]

In [171], a machine is designed in a housing of a commercially available PM-RFM. The SM-PM-CP-TFM has significantly higher torque than the PM-RFM (+50.5% in non-field weakening area). This advantage is decreasing with increasing speed demand (-9.5% at 3000min^{-1}). Yet, the specific tangential force σ of the TFM is -42.5% lower compared to the RFM due to the difference of material properties (TFM: SMC, RFM: laminated electrical steel) and the saturation at a lower magnetic flux density. Nevertheless, the torque of the TFM is higher because of a better utilization of volume and

a larger air gap diameter for equal active diameters d_a of the stators.

3) MOTOR FOR ELECTRIC VEHICLE WITH LIMITED AXIAL LENGTH [215]

A FEA based comparison of Permanent Magnet Synchronous Motors (PMSMs) as RFM, AFM and CP-TFM is examined in [215]. The machines have the same mass of PMs and installation space. The TFM is beneficial especially in low-speed operating points over a broad range of torque. Due to high electrical load the SMC of the TFM is saturated earlier compared to RFM made of electrical steel. The AFM is in the highest and widest area of high efficiency (see Fig. 6). Possible reasons for the superior properties are the double-sided air gap of the AFM, the geometrical constraints with a ratio of $d_a/l_a = 4.0$ which are atypical for a TFM (for reference see Table 2) and the inner-rotor TFM-design of the study. Measurements of the prototype of the AFM are presented in [107].

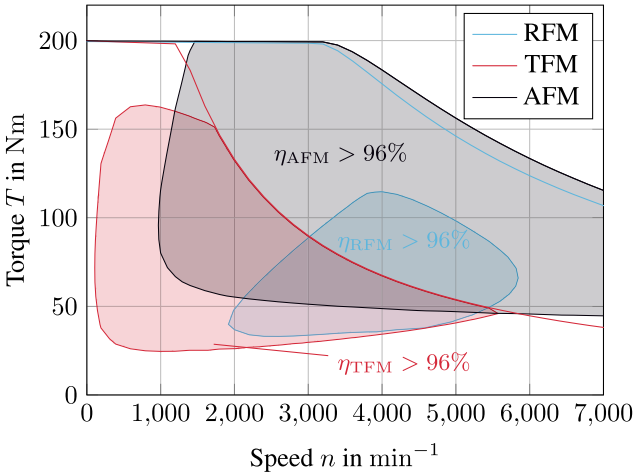

FIGURE 6. Comparison of efficiency in dependence of operation point of PMSMs as RFM, AFM, and TFM, based on [215]. Operating range of the machines is outlined with solid lines, highlighted areas represent efficiency $\eta > 96\%$. The geometrical conditions with a ratio of $d_a/l_a = 4.0$ are atypical for the design of the TFM.

4) IN-WHEEL MOTOR [47]

Similarly, in [47], a comparison of RFM, AFM, and TFM for an application as in-wheel motor with limitations in installation space and inverter limits is presented. Analytical calculations show a superiority of the TFM in torque density and efficiency with a significant lower PM mass. Only the low power factor is disadvantageous. A FEA reveals three-dimensional leakage and saturation effects in SMC, reducing the peak torque to only 46.7% of analytical prediction. Considering the results from the FEA, the TFM is inferior to the RFM and the AFM.

5) TURRET APPLICATION WITH HIGH DIAMETER [224]

For an application with a high diameter (1.6m), the TFM is disadvantageous compared to an RFM regarding efficiency with similar torque density. The immense copper losses of the TFM (0.6kW vs. 16.8kW) [224] are notable.

6) POWER TOOL APPLICATION [95]

By comparing an outer-rotor-RFM with a TFM of similar installation space, in a measurement [95] the TFM has a 40% higher steady-state torque T_{max} at the same thermal limit.

7) SPACECRAFT APPLICATION [20]

Comparing a SM-PM-TFM to BLDC-RFMs simulative, the TFM has the higher power density as well as torque density [20].

8) DOWNHOLE APPLICATION [225]

In [225] PM-RFM, -AFM and -TFM are compared, concluding that the TFM has a high efficiency and a superior torque density which is suited for low speed application. The RFM has a better power factor, a simple construction, and is suited for high speed application.

9) WIND TURBINE GENERATOR [54]

For a direct drive wind turbine generator, [54] analytically compares multiple PM-TFM-concepts with a PM-RFM, thereby displaying a superior design of the TFM with regards to copper losses, power, torque, mass, and cost.

10) 10kW-MACHINES [226]

In [226], an RFM, AFM, and an SM-PM-UI-TFM with the same power rating are compared. The RFM and AFM are optimized by an analytical tool in combination with an genetic multi-objective optimization. For the TFM, a single design without optimization is considered. The RFM outperforms the AFM and the TFM in torque density and efficiency. The TFM has a higher efficiency than the AFM but a lower torque density.

11) ROBOTICS APPLICATION [170]

The machine designed in [170] is compared to commercially available machines with a similar power rating. In Fig. 7, the torque density $\tau_{t,N}$ in dependence of nominal output power P_N of the machines is graphically represented. The Brushless DC-Machines with a torque density superior to the TFM are frame-less and therefore offer a high gravimetric torque density. For the TFM peripheral weight like the housing is included ($\tau_{t,N}$ of $0.95\frac{\mathrm{Nm}}{\mathrm{kg}}$). Considering only the active parts, the TFM has a torque density $\tau_{a,N}$ of $1.78\frac{\mathrm{Nm}}{\mathrm{kg}}$, which is higher than that of all its competitors. The Hybrid-Steppers (HSs) have a lower power density ($13\frac{\mathrm{W}}{\mathrm{kg}} - 87\frac{\mathrm{W}}{\mathrm{kg}}$) than the TFM ($148.8\frac{\mathrm{W}}{\mathrm{kg}}$).

12) SUMMARIZED STATEMENT

In Table 1, the statements of multiple comparisons are summarized. The comparisons show that there is potential to increase the torque density and the efficiency due to the

transverse flux design. However, it is challenging to select and optimize a suitable design.

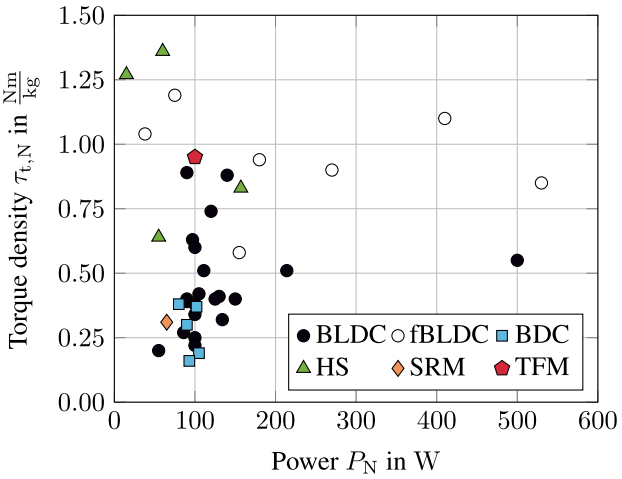

FIGURE 7. Torque density $\tau_{t,N}$ in dependence of nominal output power P_N of commercially available brush-less DC-machines (BLDC), frame-less brush-less DC-machines (fBLDC), brushed DC-machines (BDC), hybrid-steppers (HS), switched reluctance machine (SRM), and prototype TFM, based on [170].

TABLE 1. Summarized statements about comparisons of different machine principles.

Compared machines			Results of TFM				Ref.
TFM	RFM	AFM	Torque		selected characteristic		
SR-U	SR		+50%	T	−33%	V_{Cu}	[111][b]
SM-PM-CP	SM-PM		+50.5%	T	−42.5%	σ	[171][b]
FC-PM-CP	PM	SM-PM	+5.28%	T	−72.46%	P	[215][c]
SM-PM	SM-PM	SM-PM	−61%	T_{max}	+470%	T_{ripple}	[47][c]
SM-PM-U	SM-PM		+3.45%	T/m	+2812.75%	$P_{Loss,Cu}$	[224][c]
SM-PM-CP	SM-PM		+40.39%	T	+13.22%	T_{max}	[95][b]
SM-PM-U	BLDC		+74%	T	+87.63%	T_{ripple}	[20][c]
SM-PM-U	SM-PM	SM-PM	+38.35%	T	−36.55%	$\cos(\varphi)$	[225][a,c]
FC-PM-C	SM-PM		+46.86%	T/m	−44.73%	€	[54][c]
SM-PM-UI	PM	PM	−31.68%	T/V		-	[226][c]
SM-PM-CP	SM-PM		+28.4%	T/m	−22.4%	P/m	[170][b]

[a] Estimate based on longest machines with highest pole number.
[b] Based on measurements.
[c] Based on simulations.

D. COMPARISON OF TFMs

There are many options for the design of TFMsn, each of them with their own characteristics.

1) CORE-STRUCTURE

In [131], a U-structure is compared to a UI-structure. The UI-structure achieves significantly higher torque. Similarly, a comparison in [160] outlines a performance which is two times better with the additional I-core. By comparing the C-core versus the U-core geometry after an optimization process, the design of the C-core obtained a 10.5% lower mass of active materials and a 5.56% higher specific tangential force [59]. Similar results for the superiority of C-core TFM are obtained in [53]. The Z-core TFM is disadvantageous compared to U-core type of same dimensions and ratings [192] because of considerable leakage flux. In [48], CP-structure is compared with a U-structure , giving a higher torque density for the CP-TFM.

2) MATERIALS FOR FLUX GUIDANCE

The influence of the used materials for flux guidance is discussed in section IV.

3) PROTOTYPES

Table 2 presents a collection of data of Prototype-TFMs provided by the literature. The classification is conducted according to section II. There is a distinction between maximum (max) and nominal (N) values relating to active mass m_a and total mass m_t. Further, torque density τ is differentiated in gravimetric and volumetric (V). The specific tangential force σ relates to the cylindrical air gap surface of active length l_a and air gap diameter d_δ, the force is calculated with the lever arm $d_\delta/2$.

Due to the enormous scope for designing the machines and the limited number of prototypes, no reliable statements about the interrelationships are possible. In general, there is a correlation between an increased torque density and an increased total torque or power. This also applies to other types of machines. Machines with polepair-numbers p in the range of 32-40 have the highest torque density. The best ratio of d_a to l_a for a high torque density seems to be in the range of 1.04 to 1.85.

TFMs with torque higher than ≈ 80Nm are preferably built with U/UI/C-cores, for lower torque the CP-core is preferred (see Fig. 8). Stators with CP-cores are (with the exception of the machine in [35], [227] which is assembled out of part-shells) built by single shells of SMC which are limited in size. Stators with U/UI/C-cores are usually assembled of multiple core-elements. This is a possible reason for the choice of core-structure in dependence of torque and thus the size of the machine.

IV. INFLUENCE OF SOFT-MAGNETIC-MATERIALS

The most popular soft magnetic materials for construction of electrical machines are laminated electrical steel sheets and Soft-Magnetic-Composite (SMC), which differ in magnetic saturation, hysteresis, and frequency dependent losses.

Typically, SMC has a lower relative permeability and is saturated at a lower magnetic flux density compared to electrical steel. Due to its micro-structure, SMC has a high specific electric resistivity compared to electrical steel. Therefore, the utilization of SMC is beneficial at higher operating frequencies >1000Hz, whereas electrical steel is limited due to increasing eddy current losses [36], [234].

Unconventional approaches such as amorphous steel constructions [235], [236] promise an increase in efficiency due to the low magnetic losses, which are particularly significant at high speeds. Due to its low prevalence, this approach can be disregarded in the following.

The influence of the material properties on the design of the machine will be presented below. However, a detailed comparison of the material properties is not discussed here,

TABLE 2. Overview of prototypes of rotating TFMs.

Number	Nom. torque	Max. torque	Nom. power	Max. power	Nom. total torque density	Max. total torque density	Nom. active torque density	Max. active torque density	Nom. total vol. torque density	Max. total vol. torque density	Nom. active vol. torque density	Max. active vol. torque density	Nom. specific tangential force	Max. specific tangential force	Pole-pairs	Efficiency	Active mass	Total mass	Active length	Total length	Air gap diameter	Active diameter	Total diameter	Excitation	Core-structure	Rotor material	Stator material	Year	Reference
-	T_N	T_{max}	P_N	P_{max}	$\tau_{t,N}$	$\tau_{t,max}$	$\tau_{a,N}$	$\tau_{a,max}$	$\tau_{t,N,V}$	$\tau_{t,max,V}$	$\tau_{a,N,V}$	$\tau_{a,max,V}$	σ_N	σ_{max}	p	η	m_a	m_t	l_a	l_t	d_δ	d_a	d_t	-	-	-	-	-	-
-	Nm	Nm	kW	kW	$\frac{Nm}{kg}$	$\frac{Nm}{kg}$	$\frac{Nm}{kg}$	$\frac{Nm}{kg}$	$\frac{kNm}{m^3}$	$\frac{kNm}{m^3}$	$\frac{kNm}{m^3}$	$\frac{kNm}{m^3}$	$\frac{kN}{m^2}$	$\frac{kN}{m^2}$	-	%	kg	kg	mm	mm	mm	mm	mm	-	-	-	-	-	-
1	300	350[b]	17	N/A	N/A	N/A	11.82[a]	13.79[a]	N/A	N/A	27.46[b]	32.03[b]	16.19[b]	18.89[b]	40	91	25.38	N/A	180	298	256[b]	278[b]	335	SM	UI	Lam.	Lam.	1997	[228]
2	400	N/A	25	N/A	N/A	N/A	18	N/A	12.88[a]	N/A	46	N/A	25.44[a]	N/A	40	89	22.6	N/A	115	260	295	317	390	FC	U	SMC	SMC	2002	[229]
3	1.14	1.37	0.18[a]	0.22[a]	N/A	N/A	1.78[b]	2.14[b]	N/A	N/A	9.36[a]	11.25[a]	7.14[a]	8.58[a]	8	N/A	0.64[b]	N/A	62	N/A	40.5[a]	50	N/A	SM	CP	N/A	SMC	2002	[95]
4	96.46[a]	112.53[a]	6	7	N/A	N/A	4.13[a]	4.82[a]	6.77[a]	7.9[a]	9.77[b]	11.39[b]	6.39[b]	7.46[b]	18	92	23.34	N/A	222[b]	295[a]	208[b]	238[b]	248	SM	UI	Lam.	Lam.	2005	[159]
5	3.4	N/A	0.64	N/A	N/A	N/A	N/A	N/A	3.58	N/A	N/A	N/A	3.54[a]	N/A	20	79.5	N/A	N/A	93	137	81[a]	94	94	SM	U	Solid	SMC	2006	[223]
6	N/A	1000	N/A	10	N/A	6.06[a]	N/A	N/A	N/A	20.47[a]	N/A	48.46[a]	N/A	30.75[b]	37	92	N/A	165	230	270	300[b]	338	480	FC	C	SMC	Lam.	2007	[128], [230]
7	10	22	0.52[a]	1.15[a]	1.37[a]	3.01[a]	N/A	N/A	4.92[a]	10.83[a]	N/A	N/A	N/A	N/A	32	N/A	N/A	7.3	N/A	123	N/A	N/A	145	SM[b]	U[b]	N/A	N/A	2008	[231][c]
8	14	34	0.73[a]	1.78[a]	1.56[a]	3.78[a]	N/A	N/A	5.61[a]	13.64[a]	N/A	N/A	N/A	N/A	32	N/A	N/A	9	N/A	151	N/A	N/A	145	SM	U[b]	N/A	N/A	2008	[129], [231][c]
9	25	50	0.65[a]	1.31[a]	1.75[a]	3.50[a]	N/A	N/A	5.81[a]	11.62[a]	N/A	N/A	N/A	N/A	44	N/A	N/A	14.3	N/A	137	N/A	N/A	200	SM[b]	U[b]	N/A	N/A	2008	[231][c]
10	35	75	0.92[a]	1.96[a]	2.01[a]	4.49[a]	N/A	N/A	6.75[a]	14.47[a]	N/A	N/A	N/A	N/A	44	N/A	N/A	16.7	N/A	165	N/A	N/A	200	SM[b]	U[b]	N/A	N/A	2008	[231][c]
11	8681	N/A	50	N/A	7.25	N/A	N/A	N/A	25.84[a]	N/A	N/A	N/A	N/A	N/A	70[b]	N/A	N/A	1200	N/A	500	N/A	N/A	925	FC	U	SMC[b]	Lam.	2010	[60], [62]
12	N/A	80	20	44	N/A	7.84[a]	N/A	22.86[a]	N/A	N/A	N/A	N/A	N/A	30.24[b]	40	93[b]	3.5	10.2	51.4	56	181[b]	188[b]	206[b]	SM	CP	-	SMC	2011	[35], [227], [232]
13	N/A	7.45	N/A	0.22[a]	N/A	N/A	N/A	1.82	N/A	N/A	N/A	7.55[a]	N/A	4.46[a]	50[b]	N/A	3.89	N/A	49.6[b]	N/A	146.4[a]	159.2[b]	N/A	FC	U	SMC	SMC	2012	[97], [103]
14	N/A	8.92	N/A	0.27[a]	N/A	N/A	N/A	2.01	N/A	N/A	N/A	9.03[a]	N/A	5.34[b]	50[b]	N/A	4.06	N/A	49.6[b]	N/A	146.4[b]	159.2[b]	N/A	FC	U	SMC	SMC	2012	[97]
15	0.7	2	0.02[a]	0.04	0.22[a]	0.63[a]	0.68[a]	1.93[a]	0.43[a]	1.22[a]	2.06[a]	5.89[a]	1.66[a]	4.75[a]	13	53	1.04[b]	3.2	40	101	81.88	104	144	FC	E	SMC	Lam.	2013	[187]
16	400	600	5.53[a]	8.29[a]	6.15[a]	9.23[a]	11.7	17.5	26.87[a]	40.31[a]	53.49[a]	80.23[a]	30.04[a]	45.07[a]	34	70	34.3	65	180	260	217[a]	230	270	FC	U	Lam.	SMC	2014	[233]
17	10.28[b]	28.9	1.58[b]	2.98[b]	1.27[a]	3.6	N/A	N/A	5.2[a]	14.61[a]	12.75[a]	35.84[a]	17.75[a]	49.91[a]	10	90[b]	N/A	8.1	90	190.5	64	106.8	115	SM	CP	Lam.	SMC	2015	[171]
18	0.8	1.17[a]	0.1	N/A	0.95	N/A	1.78	N/A	3.61[a]	5.26[a]	10.42[a]	15.17[a]	8.10[a]	11.86[a]	12	82	0.45	0.84	34.8	61	42.5[a]	53	68	SM	CP	Lam.	SMC	2016	[170]
19	N/A	N/A	N/A	<160	N/A	N/A	24.5	N/A	N/A	N/A	N/A	N/A	N/A	N/A	32	N/A	N/A	N/A	N/A	207[b]	N/A	180[b]	396[b]	FC	U	SMC	Hyb.	2018	[17]
20	N/A	N/A	N/A	<160	N/A	N/A	19.2	N/A	N/A	N/A	N/A	N/A	N/A	N/A	32	N/A	N/A	N/A	N/A	207[b]	N/A	180[b]	396[b]	FC	U	SMC	Lam.	2018	[17]

[a] Calculated from given values.
[b] Estimated based on graphics or interpretation of images.
[c] From datasheet of series product, not a prototype.

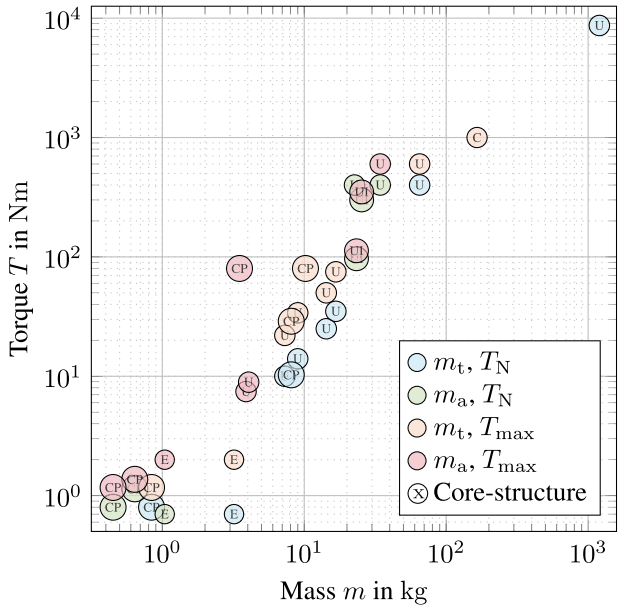

FIGURE 8. Nominal torque T_N or maximum torque T_{max} in dependence of total mass m_t or active mass m_a with the additional information of the core-structure of prototype TFMs, based on Table 2.

for further information regarding the application in electrical machines please refer to [36], [234].

A. LAMINATED-STEEL MACHINES

Due to the anisotropic magnetic properties of laminated electrical steel sheets [237], the lamination has to be oriented according to the direction of the flux, which results in a complex mechanical design. The assembling technologies of TFMs used with traditional laminated steel are classified in the following methods:

1) ADAPTED DESIGN FOR TWO-DIMENSIONAL LAMINATED STEEL

These designs [11], [153]–[155], [159], [238] enable the utilization of electrical steel with beneficial magnetic properties, but highly limit the design possibilities. An example is illustrated in Fig. 9. Because of the forces occurring between these elements, the construction has to be reinforced with paramagnetic materials [159].

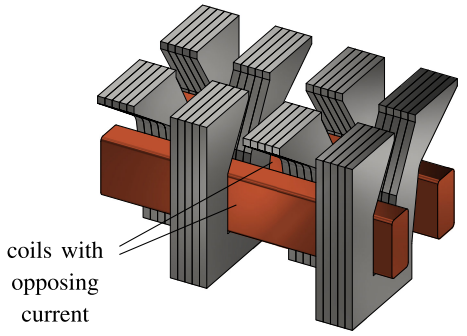

FIGURE 9. Concept of 2D laminated electrical steel assembled and reinforced with a paramagnetic carrier (not illustrated), based on [154].

2) 3D ASSEMBLY OF LAMINATED STEEL SUB-ASSEMBLIES

For the 3D assembly with smaller 2D sub-assemblies [38], [40], [119], [148], [239], [240] (see in Fig. 10) it is important to have an electrical insulation between the packages.

Damaged insulation causes significant eddy current losses [233].

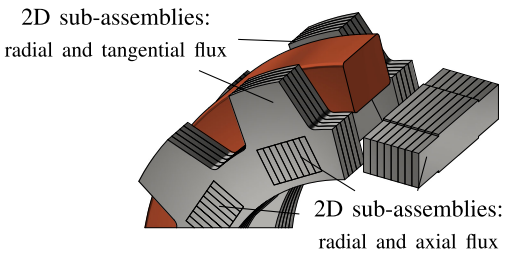

FIGURE 10. Concept of 3D assembly of laminated electrical steel sub-assemblies, based on [148].

3) BENDING OF STEEL SHEETS

Especially machines with bend laminations [17], [99], [100] (see in Fig. 11) are challenging to manufacture in compliance with the required tolerances [99]. There are multiple problems contributing to the complicated manufacturing process. Firstly, the magnetic properties are influenced by the manufacturing process [36]. Furthermore, space-efficient combined phase topology (topology in [97]) is not manufacturable [17]. Most importantly, due to the different bending radii of each layer, the steel sheets tend to fan out [100].

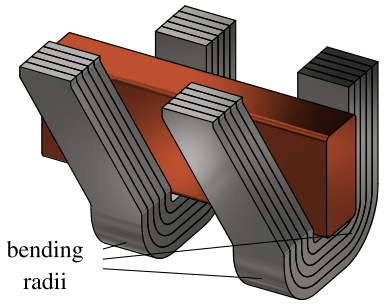

FIGURE 11. Lamination concept of bend electrical steel sheets, based on [17].

4) COMBINATION OF LAMINATED STEEL AND SMC

The hybrid-type [17], [18], [21], [110], [111], [166], [184], [210] (see in Fig. 12) is a very promising concept, enabling the utilization of both beneficial properties. However, the SMC limits the overload capability of the machine because of the low magnetic saturation level of the material [17] which is a drawback of this concept.

B. SMC-MACHINES

Pure SMC-flux-path machines can for instance be found in [34]–[36], [42], [178], [210], [241], [242]. In general, the design of the machine has to be adapted in order to benefit from the properties of SMC [36]. In contrast to the anisotropic magnetic properties of laminated electrical steel sheets, the isotropic SMC material allows the design of complex geometries [210], [243]. The utilization of SMC

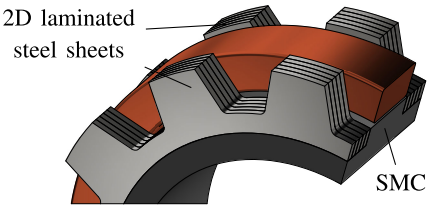

FIGURE 12. Hybrid lamination concept with a combination of laminated steel and SMC, here with laminated teeth (light gray) and SMC-yoke (dark gray).

shows a great potential for machines with complex three-dimensional flux paths and structures [244]. The freedom in the three-dimensional design of SMC components allows the utilization of optimization strategies for a beneficial torque density due to a better material utilization. In [92], a complete design and optimizing process of a SMC-TFM is presented in an analytical and numerical way. The geometry optimization process to achieve a constant distribution of flux density is outlined. Further, the well-known optimization strategy of Tensile Triangles used in the field of mechanics in order to reduce notch-stress allows to reduce induction fluctuations significantly. Faults in the distribution of density of the pressed powder may occur in the manufacturing process lead to partial saturation affecting the flux distribution [210].

Further, SMC has the enormous disadvantage of a low mechanical tensile strength. On the one hand, due to brittleness the material breaks when subjected to shock loads, especially in thin sections [238]. For a higher mechanical strength of the system, SMC is often casted in resin with high mineral percentage for good heat dissipation [232]. On the other hand, the brittleness simplifies the separation of materials in disassembly and recycling processes [90].

Prototyping with SMC is difficult seeing as the expensive pressing tool is not suited for single piece production. Milling of a semi-finished blank product made of prototyping material is possible, but restrictions in design impede congruence with a series product. Faults in geometry, such as damaged corners and edges, occur due to the machining process [245], [246].

C. COMPARISON OF LAMINATED-, HYBRID- AND SMC-MACHINES

A comparison of laminated, hybrid or full-SMC machines is given in [17], [99], [247]. In [17], a hybrid machine with laminated and SMC yoke is compared to a bend laminated machine. Prototypes have shown that the torque density of the hybrid machine ($24.5^{\mathrm{Nm}}/_{\mathrm{kg}}$) is 27.6% higher than the bend lamination machine ($19.2^{\mathrm{Nm}}/_{\mathrm{kg}}$) at rated current density of $6.5^{\mathrm{A}}/_{\mathrm{mm}^2}$. In [99], compared to a full SMC machine, a hybrid-type has a 12% and a laminated-type has a 33% higher torque density.

Regarding the cost of the machine, the material costs per kg of SMC are approximately three times higher compared to laminations [248]. Manufacturing processes of SMC with mixing of material, pressing within a tool, and thermal

treatment [37] are suited for higher lot productions. Therefore, SMC is competitive with laminated machines in applications where cost and size are important [90]. Especially the low number of parts required for the assembly of the stator offers reduced manufacturing cost [223]. Compared to a punching tool for production of steel sheets with an estimated cost of 200, 000€, the pressing tool is about 25, 000€ to 70, 000€, depending on the geometry of the part [248]. The pressing process has the additional advantage of not generating scrap material [90]. In addition, for an AFM it is shown how the utilization of an intelligent design by the use of SMC the size and thus the cost of the motor could be reduced compared to a laminated machine with standard design [248].

D. ADDITIONAL DESIGN TECHNIQUES

In reviewed papers several suggestions are illustrated for an optimum design of the machine which depend on the choice of materials and the associated opportunities.

1) PREVENTION OF CIRCUMFERENTIAL EDDY CURRENT

To eliminate additional losses especially for laminated machines there has to be a gap avoiding a closed electrically conductive path, preventing the flow of induced eddy current in circumferentially direction [18], [110], [247] as shown in Fig. 13. With this simple change in design, the core losses are significantly reduced [247].

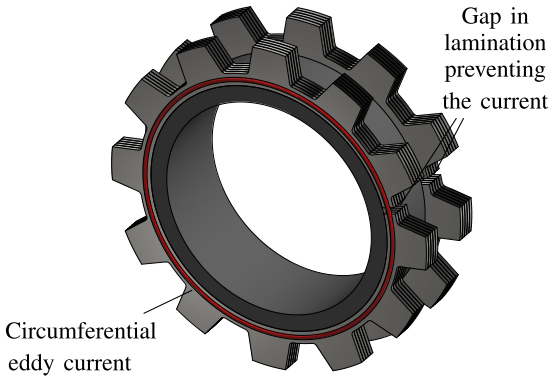

FIGURE 13. A gap in the lamination of electrical steel sheets (gray) breaking circumferentially current (red) around the rotation axis which is induced by mechanical and magnetic inaccuracies, based on [110].

2) ELECTRICAL RESISTANCE OF THE COIL

Another suggestion is based on the electrical resistance of a ring coil which is increasing with diameter. Therefore, an outer rotor design with a smaller diameter of the ring winding is beneficial regarding the conductive losses [249].

3) OUTER ROTOR DESIGN

A further advantage of an outer rotor design is the better ratio of air gap diameter to outer diameter because of a typically thinner rotor compared to the thickness of the stator [145]. This results in a higher torque density because of the larger air gap diameter.

4) CARRIER MATERIALS

With the typically highly saturated soft-magnetic parts causing leakage flux at high operating frequencies, eddy currents are induced in electrically conductive parts. Therefore, aluminum carriers are not suited for the construction of TFMs because of the high additional losses as discussed in [145], [228]. Another example of a prototype with unacceptable losses in the aluminum carrier is given in [187]. Here, the rotor losses are equal to 40% of the power defined by the air gap based on results of a FEA. In conclusion, non-conductive materials have to be used or the leakage has to be reduced. [221], [250] point out the problems and resulting requirements of the carriers. These consist of high stiffness, high thermal conductivity, and electrical insulation. In order to reduce noise, the core-structure is embedded in vibration dampening polymer. For the prototype in [251], an Aluminum Oxide Ceramic is used as an alternative to metal construction.

5) MAGNETICALLY COUPLED PHASE DESIGN

Eliminating the magnetic insulation between the single phases in [229] and [97] a magnetically coupled concept with a combined flux-path is presented (see Fig. 14). Compared to a magnetically decoupled machine of the same size, prototypes with the same thermal limit have shown that the combined flux-path machine has a 10.4% increased gravimetric torque density [97]. In addition, the total number of SMC components of a three phase machine is decreased from six to four, with the drawback of non-identical geometries.

6) STATOR SEGMENTATION

The segmentation of single phases into phase segments as presented in [52], [92] is beneficial regarding the torque density and the amount of used of soft magnetic material. The basic idea is to shorten the flux path and to increase the air gap diameter preserving geometrical boundary conditions while keeping the copper area constant (see Fig. 15). By separating a single phase segment into two segments per phase, the volumetric torque density is nearly tripled [92]. However, there is a balance between the increase of the torque density and the effort in production due to the number of parts.

7) STACKING DIRECTION OF PHASE-SEGMENTS

Furthermore, leakage flux may be taken into consideration. In order to prevent leakage flux between the segments of a phase, an optimized stacking direction has to be considered [93]. Additionally, in [93], the stacking sequence of the phases is optimized in order to reduce the leakage flux between the phases resulting in a magnetically coupled-phase design with identical geometries.

8) ANGULAR ERRORS IN MANUFACTURING

Due to component tolerances, angular errors add up when individual components are arranged and assembled

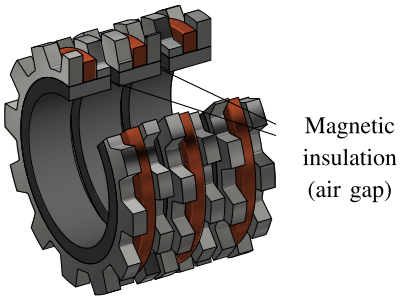

(a) Magnetically separated-phase design

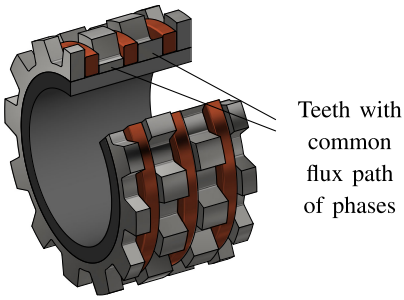

(b) Magnetically coupled-phase design

FIGURE 14. Magnetically separated-phase design transformed in a magnetically coupled-phase design with a common flux path, based on [97].

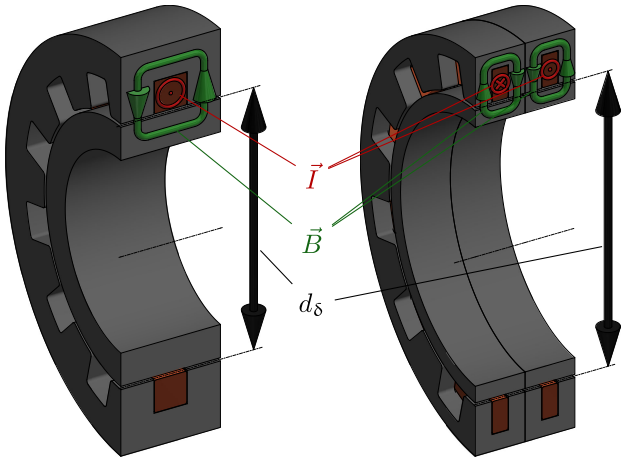

FIGURE 15. Segmentation of a single phase element into multiple (illustrated: two) elements with multiple coils. Due to this design, air gap diameter d_δ is increased, while copper area and geometrical constraints (active diameter d_a and active length l_a) is keept constant. In addition, the length of flux path is decreased.

circumferentially. For FC-PM-TFM this typically occurs during assembly of the alternating soft magnetic and hard magnetic parts of the rotor assembly [252]. In order to avoid those errors, appropriate measures have to be implemented in design and production.

V. MODELING OF TFMs

Diverse modeling technologies are used to predict the behavior during the early design phase, optimization process and operation. An overview of the modeling methods used for the TFM is provided in the following.

A. ANALYTICAL PRELIMINARY DESIGN

There have been various attempts and approaches to describe TFMs with convenient analytical equations [8], [11], [149]. Due to the nonlinear characteristic, which result from the saturation of the soft magnetic material and the complex three-dimensional flux, some authors consider this as challenging or even impossible [188], [253].

In [217], a complete electromagnetic design procedure is purposed with a separation in two parts: an analytical estimation and an optimization by 3D-FEA. The estimation is conducted with the help of sizing factors known from experience with previous prototypes.

In comparison with conventional machines for which the fundamental wave of the magnetic flux density $B_{1,\delta}$ is used to estimate torque or induced voltage. This is not accurate for TFMs because of the significant leakage flux. It is suggested to use the maximum flux density of the saturated material $B_{\max}$ and a factor ${}^{\tau_S}/_{\tau_P}$ considering angle of stator tooth τ_S and pole pitch τ_P to estimate a $B_{1,\delta}$-value [163].

In [254], a leakage per unit factor is introduced for a qualitative analysis which is proportional to the number of pole pairs and inverse proportional to the length of the air gap.

B. MAGNETIC EQUIVALENT CIRCUIT

In order to obtain an accurate analytical model, the Magnetic Equivalent Circuit (MEC) using Hopkinson's law to represent the main flux paths of the machines. MEC-modeling of TFMs is found in many publications, conducted via the reluctance [9], [56], [155], [194], [227], [229], [239], [241], [249], [255]–[259] or via the permeance [1], [67], [117], [119], [148], [260], [261] of magnetic circuit.

The flux distribution of the machine is difficult to describe analytically. In order to solve this problem, one solution which arises is the modeling via flux tubes, approximating the flux-paths as presented in [1], [220], [261], [262].

An advanced solution is presented in [119], [170]. Using the Schwarz-Christoffel integral, a conformal mapping of the simplified air gap is discussed, resulting in a semi-analytical calculation of the air gap flux density, thus achieving good results compared to a FEA.

In [148], a laminated FC-PM-TFM is modeled by segmentation in five planes perpendicular to the rotation axis, considering saturation by adapting the permeability of the corresponding elements.

In [227], [256], the reluctance of complex geometries, including the claw structure and stray fields, is adjusted to reference data obtained from FEA and measurements. The influence of the saturation is included, resulting in an iterative computation.

The leakage flux is difficult to model with a MEC and therefore often neglected. This results in an offset to numerical solutions which increases with the current due to the

increasing leakage in combination with the saturation of the soft magnetic material [119]. In [148], the leakage is modeled by additional permeances defined by Flux-Tubes. The MEC is solved via nodal analysis, afterwards calculating the torque via virtual displacement. The model is solved in only 6s, which is significantly faster than FEA. In comparison to FEA, the solution via MEC provides good results for low currents of the stator-winding. For high currents, the results show the weakness of coarse modeling by MEC. In this operating point the influence of locally high saturation of soft magnetic material is not represented, which leads to divergent Flux-Tubes compared to the initial definition MEC-model [233].

C. GYRATOR-CAPACITOR-MODEL

Similar to the previously presented approach, the Gyrator-Capacitor-Model (please find the basics in [249]) is used to describe the TFM analytically with an equivalent circuit of electrical elements. This approach has the major advantage of the calculation of Maxwell's force including influence of saturation of soft magnetic material [249]. This is especially important for TFMs, which typically have strongly saturated soft magnetic parts. In comparison to MEC, magnetically stored energy is modeled in the GyCap-Model [249]. The MEC is still used as basis for building the GyCap-Model by transferring single components into the new approach [263]. In [249], [263], an analytical GyCap-Model for the hardware emulation of a TFM is presented and compared to measurements.

D. MAGNETIC CHARGE AND IMAGING

The publications [78], [264]–[269] present a semi-analytical computation of a SM-PM-TFM, based on a combination of the model of magnetic charge and the method of images. The force is calculated by the Lorentz force method, using a modified but equivalent coil layout. The modification is necessary in order to compute the Lorentz-Force analytically. This model has an error rate of 10% related to the magnetic flux density in the air gap compared to an FEA and 15% related to electromotive force (EMF) compared to measurements [264]. The semi-analytical computation is 51.7 times faster than the FEA. Said error rate in [264] could be reduced by using an iterative approach [269]. Disadvantages of the method is the usage of magnetostatic equations. Therefore, it is not possible to calculate the transient behavior of the machine [78].

E. FINITE ELEMENT ANALYSIS

Due to the complex flux path, the 3D-FEA is mainly used for the prediction and optimization of the behavior of the investigated arrangement. Therefore, this method is utilized in several publications (e.g. in [60], [158], [183], [185], [193], [237], [253], [255], [270]–[280]). With this calculation, leakage flux is investigated [163] and the influence of nonlinear and anisotropic properties of the material is considered [237], thereby receiving results with good accordance on measurements. A particular advantage is the consideration of fringing and leakage flux, which have a decisive influence on machine behavior [94].

A huge disadvantage is the time consuming calculation [119]. A simulation of a design including the calculation of 19 rotor positions, for instance, has a duration of 70min [237] while already using symmetry to reduce the meshing area. Hence, the optimization processes with lots of iterations are usually very time-intensive. In [124], [281], an equivalent 2D model for a fast calculation is described, accepting boundary effects which are not existent in a 3D model. The comparison with a 3D-FEA shows almost identical results, quantitatively -2.39% deviation in torque from 2D to 3D-FEA [281].

F. CO-ENERGY

In [282], the calculation of torque via the magnetic co-energy including saturation effects is presented. A polynomial function which approximates the flux linkage $\Psi(i)$ for the unaligned position of the rotor is obtained through a FEA, whereby the flux linkage originating from the permanent magnets is set to zero $\hat{\Psi}_{\mathrm{PM}} = 0$. The functions for the other positions are estimated by shifting the polynomial along the i-axis by a current i_{S}. The current i_{S} represents an equivalent current of PMs influencing flux linkage Ψ. The flux linkage $\hat{\Psi}_{\mathrm{PM}}$ is obtained through a FEA as well. With the help of magnetic co-energy an equation for torque is introduced. The validation by measurements show a good accordance. A major disadvantage of this method is the derivation of the initial $\Psi(i)$-curve, which must be determined by measurement or FEA. Combining the analytical model presented in [282] with [283], the calculation of the power factor $\cos\varphi$ is possible.

G. DYNAMIC LOOK-UP-TABLE-MODEL

For controller and circuit design of power electronics a dynamic model of the TFM has to be established. Because of the typically long simulation time, dynamics of every single time step are not computed via 3D-FEA. Look-Up-Table-based (LUT) models for simulations in the development of controllers for electrical machines are used for TFMs as well. The tables are parameterized by a 3D-FEA [253], [272], [284], [285] or measurements [109]. The machine behavior is defined by differential equations of motor phase, torque, and mechanics. In [284], the phases are modeled separately by tabulated data of the current $i(\Psi, \epsilon_{\mathrm{L,mech}})$ and the torque $T(i, \epsilon_{\mathrm{L,mech}})$ in dependence of the flux linkage Ψ, the rotor angle $\epsilon_{\mathrm{L,mech}}$, and the current i. The design of the control for the modeled TFM is presented in [60]. In [286], a simplified mathematical model for dynamic simulation of reluctance type TFM is proposed, but not validated through FEA or experiments.

H. DYNAMIC OBSERVER AND NEURAL NETWORK-MODEL

A high gain observer and radial basis function networks are utilized in [287]–[292] to model a FC-PM-TFM as a nonlinear system. Further, an adaptive control law is developed

in order to compensate unknown nonlinear parts. Similarly, in [188] a neural network is used to determine the dynamics of a TFM.

Neural networks are a general purpose modeling approach and therefore not limited to the modeling of the machine behavior. They are used for controller design as well. In [293] a control via a neural network in combination with a fuzzy logic controller is presented.

VI. MINIMIZATION OF TORQUE RIPPLE

The reduction of torque ripple is either achieved via a mechanical or a control approach. Popular approaches are presented in the following, starting with the mechanical solutions.

A. MECHANICAL

1) NUMBER OF PHASES

The number of phases has a direct influence on the torque characteristic of the machine. The torque of magnetically separated phases can be added by superposition-principle in consideration of the mechanical angle of the phases. For example the first harmonics of cogging torque of a 2-phase TFM are compensated by each other [249]. For a smooth total torque, additional control methods are required.

2) SKEWING

As is known from RFM, skewing of the stator or the rotor is a method for minimizing cogging torque while either lowering the performance of the machine or complicating the design [294]. Applied to TFMs, there are possibilities to skew stator-teeth [146], [295] or the rotor [166], [296], [297]. Due to the reduced gradient of magnetic reluctance with simultaneous reduced effective tooth area for torque production, the average torque is usually decreasing with this approach [146]. Seen in the results of a FEA, cogging torque could be reduced by 82% [295] or 46.68% [146], accepting a comparatively high loss of 10% [295] or 9.21% [146] of average torque, respectively.

Based on the same effect, in [218] the stator teeth are not skewed but axially tapered to achieve a lower 6^{th} harmonic, not giving quantified information about the effect.

Additionally, [298] presents a discrete skewed solution in order to eliminate specially selected harmonics. The cogging torque is decreased by 96% with this method.

3) OVERLAP OF STATOR TEETH

The overlap of the claw poles as one of the most influencing design parameters for a FC-PM-CP-TFM is investigated in [299]. By optimizing the maximum output torque and minimizing the cogging torque, an optimum value of around 30% overlap is found for this specific geometry. With an overlap of 100%, the flux linkage between stator and rotor is increased. Nevertheless, this solution is not equal to the maximum torque. This originates from an increase in leakage flux between neighboring stator teeth.

4) COMBINATIONS OF VARYING TOOTH SPAN

The tooth span (see Fig. 16) has an influence on the harmonics of back-EMF and (cogging) torque. In order to reduce these harmonics of back-EMF, cogging torque, and torque ripple in [102], an investigation is presented. First, the influence of the tooth span was examined. Subsequently, different combinations of teeth with various spans within one machine are considered, reducing cogging torque by 90% and torque ripple by 65% accepting a loss of 5% of the average torque with the selected combination referring to the 120°-tooth span basic model. An additional investigation of the combination of different tooth spans can be found in [300] with a reduction of torque ripple by 80.1% and an increase in average torque of 0.5%.

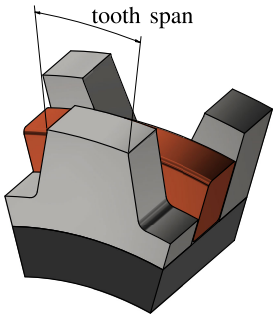

FIGURE 16. Design parameter of the tooth span of a single tooth, affecting the harmonics of back-EMF, cogging torque, and torque ripple. The tooth span and combinations of teeth with different tooth spans are used as an optimization parameter for the minimization of torque ripple.

5) SHIFT OF STATOR POLES

Further, there is the possibility to shift single pole pairs by a defined additional pitch-angle in order to suppress harmonics (see Fig. 17). In [136], this method results in an almost sinusoidal torque curve, limiting harmonics up to the 10^{th} harmonic to less than 3% of the fundamental wave amplitude. In [103], the cogging torque was reduced by 73.8% while increasing the average torque by 3.5% at the same magnetomotive force (MMF). This was conducted with the method of pitched poles, aimed to suppress the dominant 6^{th} harmonic. In addition, total harmonic distortion in Back-EMF (Line-Line) was reduced from 3.30% to only 0.64%. In [300], good results were also achieved by shifting complete stator disks. Results for the combination of variable tooth-span and pitched-poles are presented in [31], [301]. In [31], the investigation of simple, convex or wave shaped pole pieces of the rotor is added. These publications point out the enormous potential of combined small geometrical changes to specifically influence undesirable harmonics in order to tune the machine to an optimum design.

6) SKEWING OF PHASE SEGMENTS

An additional method to minimize cogging torque is the skewing of phase segments, investigated for a SM-PM-CP-TFM. In [171], [173], [302], the cogging torque of a $k = 2$

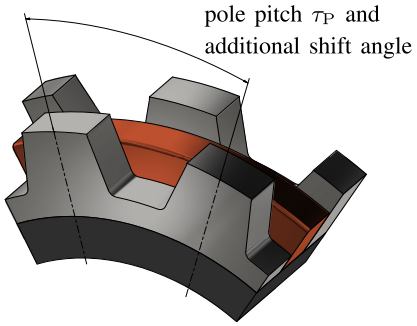

FIGURE 17. Method of an additional shift angle between the stator poles in order to suppress harmonics.

phase segmented machine was reduced by 82.9%, accepting a loss of 3.4% of the average torque compared to the non-skewed machine. The main idea is to reduce the dominating m^{th} harmonic of cogging torque by the destructive interference of the k phase segments expressed by the mechanical skewing of angle ϑ defined as in (1).

$$\vartheta = \frac{\pi}{k \cdot p \cdot m} \tag{1}$$

This method is limited by the accuracy of manufacturing with increased demands of precision within increasing number of pole pairs, phase segments or phases.

B. CONTROL-METHODS

Compared to RFMs, TFMs do not use a rotating field for torque generation but an alternating field [128]. Nevertheless, known methods for the control of synchronous machines as the Field-Oriented-Control (FOC) are applicable [83], including Maximum Torque per Ampere or Maximum Efficiency Control Strategies [303]. Even sensor-less control methods via Direct Torque Control [304] or Hysteresis Control [227] are possible. Consequently, control methods for the torque ripple minimization of conventional machines are utilized for TFMs as well.

1) CURRENT SHAPING - ITERATIVE

The approach presented in [305] could also be applied to TFMs. In this publication the generation of currents is investigated, producing torque opposite to the torque ripple of the machine. The current shape is iteratively calculated and selected by the criteria of the peak current value, additional copper losses or the current harmonic factor. The demanded high accuracy referring to the symmetry of the phases and the angle is problematic, resulting in an arduous achievement of a torque ripple of 1%. This is even more challenging for TFMs because of the small pole pitch and the additional tolerances from the assembly of the phases.

2) CURRENT SHAPING - BASED ON LOOK-UP-TABLE

A similar approach is discussed and experimentally proven for a linear TFM in [306], [307]. The current shaping is based on a Look-up-Table (LUT) providing information about the force in dependency of current and position of the single phases. The force demand of a cascaded speed controller is individually set by a force allocator to an optimum without torque ripple for each phase. With the inverted LUT, the current demand is calculated and set by a current control. Results show a highly improved dynamic behavior during a positioning task. Disadvantages are the static LUTs which have to be measured for every machine. Further, this method of controlling single phases by one H-bridge is not cost-effective for e.g. converters suitable for three phase machine designs. For a rotating two-phase FC-PM-TFM this approach is stated in [214] and for a four-phase SR-TFM in [308].

3) CURRENT SHAPING - MODEL-BASED

In [260], based on a model of a TFM built as angle-dependent equivalent magnetic circuit, the currents are calculated to result in a constant torque. Additionally, a feed-forward control of rotationally induced voltages is implemented. Harmonics are effectively reduced, but only in a limited operating range due to the limited bandwidth of the closed-loop current control.

4) BALANCING OF PHASE-CURRENTS

To take asymmetries of the machine into account, an online estimation of machine parameters and utilization of the parameters in a control with a feed-forward scheme is beneficial for the reduction of the torque ripple. In [309], this is presented for stator resistances of an RFM, significantly reducing torque ripple of the harmonic corresponding to asymmetrical phases.

VII. POWER FACTOR

A frequently mentioned disadvantage of TFMs is the power factor. Thus, this section is dedicated to discuss said topic in detail with focus on the PM-TFM in Field-Oriented-Control.

A. IMPACT OF THE POWER FACTOR

One major disadvantage of TFMs is the low power factor. Especially at high current operating points, power factors as low as 0.34 [105] may occur. The power factor $\cos(\varphi)$ is defined as ratio of real power P and apparent power S of AC systems. With a lower power factor, the power rating and the losses of the drive inverter increases [222], [310] and preserve the drive system from obtaining a high power density [16]. In order to be able to compete with other machine principles for the broad usage in applications, an estimated power factor $\cos(\varphi) > 0.7$ needs to be reached [169].

B. COMPARISON OF MACHINES

In [170], the power factor of an outer-rotor TFM for robotic applications is compared with an outer-rotor RFM used in modern robotic joints. The measured power factor $\cos(\varphi)$ of the TFM is in the range of $0.70 < \cos(\varphi) < 0.98$. Measurements show a decrease of the power factor with an increase of the torque. The RFM has a continual high power factor $0.985 < \cos(\varphi) < 1.0$ over the entire operating range.

In [171], the power factor of the TFM is directly compared to the power factor of an RFM of similar size via measurement. Both machines are operated in nominal operation, defined by the thermal limit in continuous operation. The TFM has a power factor of approx. $0.67 < \cos(\varphi) < 0.81$, slightly increasing with speed. The RFM has a power factor of approx. $0.58 < \cos(\varphi) < 0.77$ with a maximum in the speed curve. Hence, the TFM is superior.

In [48], the power factor of simulated TFMs with CP-core and U-core with different pole pair numbers is in the range of $0.18 < \cos(\varphi) < 0.23$. This is significantly lower compared to an RFM with $\cos(\varphi) = 0.86$ of the same size. However, the power factor of the TFMs is not optimized.

Materials for flux guidance have an influence on the power factor, as can be seen in [99]. By comparing a full-SMC versus a hybrid machine, the latter has a higher power factor ($\cos(\varphi) = 0.4$ vs. $\cos(\varphi) = 0.62$).

In Table 3 the power factor of different TFMs is compared, showing a large span with different results. The power factors of the considered machines are dependent on the operating point. Based on the few examples, no reliable correlation regarding the classification is identified.

TABLE 3. Comparison of the power factor of rotating TFMs.

Power factor $\cos(\varphi)$	Torque density τ in $\frac{\mathrm{Nm}}{\mathrm{kg}}$	Machine classification PM	Core	Rotor	Stator	Source	Ref.
$0.56 - 0.99$	18	FC	U	SMC	SMC	Meas.	[229]
$0.70 - 0.98$	1.78	SM	CP	Lam.	SMC	Meas.	[170]
$0.41 - 0.94$	11.82	SM	UI	Lam.	Lam.	Meas.	[228]
$0.51 - 0.93$	4.13	SM	UI	Lam.	Lam.	Meas.	[159]
$0.67 - 0.81$	3.6	SM	CP	Lam.	SMC	Meas.	[171]
$0.68 - 0.8$	N/A	SM	U	Solid[a]	Lam.	Meas.	[311]
0.71	10.49	FC	U	SMC	Lam.	Meas.	[100]
> 0.7	N/A	FC	C	Lam.	Lam.	Meas.	[162]
0.63	0.68	FC	E	SMC	Lam.	Meas.	[187]
0.62	8.16	FC	U	SMC	Hybrid	Sim.	[99]
0.60	6.06	FC	C	SMC	Lam.	Meas.	[128]
0.53	N/A	FC	C	SMC	SMC	Meas.	[105]
0.4	7.28	FC	U	SMC	SMC	Sim.	[99]
$0.34 - 0.4$	N/A	SM	C	Lam.	Lam.	Meas.	[105]
$0.20 - 0.23$	45.7	FC	CP	SMC	Lam.[a]	Sim.	[48]
$0.18 - 0.21$	47.6	FC	U	SMC	Lam.[a]	Sim.	[48]

[a] Presumably used material

C. REASON FOR THE LOW POWER FACTOR

The reasons for the typically low power factor are not uniformly described.

Many authors point to the high leakage flux of the structure as the main reason for the low power factor [78], [266], [310], [312]. For Instance, in [310] almost 80% of flux caused by the armature current is identified as leakage. Reference [159] identifies the high leakage reactance X_σ as a reason for the low power factor. For TFMs, the leakage reactance is typically higher than the armature reaction (mutual) inductances ($X_\sigma > X_{\mathrm{m,d}}$ and $X_\sigma > X_{\mathrm{m,d}}$), for well-designed PMSM the leakage reactance is generally smaller ($X_\sigma < X_{\mathrm{m,d}}$) [159]. The complex 3D-structure of the TFM with the multiple core elements allows for many possibilities for fringing and leakage flux paths, which are not occurring in conventional machines [78].

In [310], [313], not only the leakage but also the ineffective use of flux produced by the magnets is stated as an additional reason. It is demonstrated that the flux of the magnets which are not in aligned position during the rotation decrease the total flux by crossing the air gap in opposite direction to the main flux (caused by the armature current). To sum up, the low power factor is not only caused by leakage but also by electromagnetic interaction of neighboring opposing poles.

With the appearance of saturated soft magnetic parts of the stator by the flux caused by armature current in [217], an additional attempt is presented to explain the lower power factor at higher torques. In operation points of high torque, the reluctance of the flux path of the PMs increases because of the saturation due to the flux resulting from armature current. As a result, the flux linkage of the PMs decreases due to higher leakage flux and thus the induced EMF. This is confirmed by measurements [170], which show a decrease in $\hat{\Psi}_{\mathrm{PM}}$ with an increase in $i_{1\mathrm{q}}$.

D. INFLUENCES AND SENSITIVITY

With increased specific volumetric torque the machines tend to have a lower power factor [310], thus offering only limited possibilities for improvements by electromagnetic design [222], [254]. The power factor can be predicted for instance by a phasor-diagram commonly used for conventional synchronous machines [229], [310]. Assuming neglected ohmic losses and pure $i_{1\mathrm{q}}$-current in stationary operation, the power factor is calculated by (2).

$$\cos\varphi = \cos\left(\tan^{-1}\left(\frac{I_\mathrm{q} X_\mathrm{q}}{U_\mathrm{i}}\right)\right) \tag{2}$$

During operation, the power factor $\cos(\varphi)$ decreases with an increase of torque and thus with an increase of current [159], [169], confirmed with measurements [228]. Additionally, the measurements in [228] confirm the independence of rotational speed and the power factor [145], [310]. The independence from the speed is explained by the induced voltage and the stator reactance, which are both proportional to the speed [145].

An explanation for the decreasing power factor with an increase of the torque T can be found in an analysis presented in [254]. With a simplified assumption of the leakage flux, the proportionality of the torque T to the electrical loading A and the flux density in the air gap B_δ is discussed (3).

$$T \propto \cdot A \cdot B_\delta \tag{3}$$

Inversely, the product of the current I_q and the reactance X_q divided by the induced voltage U_i is proportional to the ratio of the electrical loading A and the flux density in the air gap B_δ (4). With a higher ratio of armature reactance versus

induced voltage the power factor decreases [222], [283].

$$\frac{I_{\mathrm{q}} X_{\mathrm{q}}}{U_{\mathrm{i}}} \propto \frac{A}{B_{\delta}} \tag{4}$$

Including limitations of the flux density in the air gap B_{δ} due to material properties, the further increase of the torque T is only possible with an increase of the electrical loading A and a decrease of the power factor. Similarly, in [314] an analytical model is presented pointing out the correlation between a decreasing power factor and a rising specific tangential force for the same PM excitation.

Other designs, such as the combined phase design, illustrated in Fig. 14b, improve the torque density but increase the inductance of the machine, leading to a negative impact on the power factor.

E. IMPROVEMENT OF POWER FACTOR

As stated previously, the optimization of the power factor by electromagnetic design with a simultaneous high torque density is limited. In [313] it is mentioned that the reason for the low power factor is often a focus on the torque density during the optimization process, neglecting the power factor. This is substantiated by the study [313], which shows that in regions of high torque a small increase in torque results in a high loss of the power factor. This is schematically represented with Fig. 18. The with the number of the pole pairs initially increasing torque-curve reaches a maximum and decreases again. The curve of the power factor continuously decreases with an increase of the pole pair number. In conclusion, small losses in the torque density have a high impact on the power factor. For the influence of single-design parameters with analytically computed effects, please refer to [255].

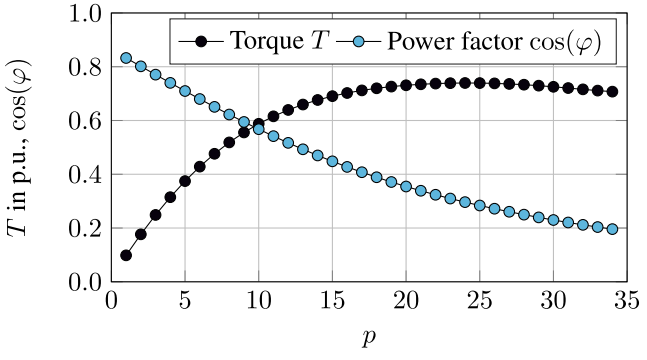

FIGURE 18. Qualitative curves of torque T and power factor $\cos(\varphi)$ in dependence of pole pairs p, based on data given in [313].

Improved control methods offer additional opportunities. Not directly improving the power factor but the impact on the converter rating, the operation mode of the converter in [13] is switched from sinusoidal to trapezoidal operation above 80% of the maximum speed. This allows for a reduction of the converter rating.

With an additional direct-axis current $i_{1\mathrm{d}}$, the power factor is influenced and enhanced, even in the typically non-field-weakening area. Due to the weakened field of the permanent magnets causing significant lower iron-losses with a small increase in ohmic losses from the additional current, the efficiency is improved as well [229]. This influence is analytically discussed in [283].

In order to gain an additional degree of freedom, an electrical excited TFM or a mechanical solution [315] may be beneficial regarding the power factor. Due to a variable induced voltage by the controllable rotor excitation, the power factor is adjustable. This statement has to be validated in future research.

VIII. CONCLUSION

Within this work, an extensive state of the art relating to Transverse Flux Machines (TFMs) is summarized in a concise form. The superiority of the TFM strongly depends on the specific applications. Especially in direct drive applications with a demand of a high torque at low speeds, TFMs demonstrate advantages. Consequently, the operation in the generator mode for renewable energies or the motor operation in the mobility-, robotics-, and automation field are important areas of applications.

The high torque density and efficiency are confirmed by various prototypes. The disadvantage of a high torque ripple is handled by methods of mechanical design and control.

The mechanical assembly, the complex system behavior, and the low power factor at high torque output are challenges which still require satisfactory solutions. The usage of Soft-Magnetic-Composite enables a modular power-scaled concept for the series production with the disadvantage of a low torque overload capability. Even today, niche applications are feasible. The improvement of the power factor is physically limited by the Soft-Magnetic-Material and could be seen as trade-off between this and the torque density. Additional possibilities are offered by control methods or new materials. There is still a need for research in relation to manufacturing methods, materials, and modeling methods for a faster optimization. Differences in the thermal behavior of these machines are insufficiently studied and offer additional potential.

REFERENCES

[1] A. Babazadeh, N. Parspour, and A. Hanifi, "Transverse flux machine for direct drive robots: Modelling and analysis," in *Proc. IEEE Conf. Robot., Automat. Mechatronics*, Dec. 2004, pp. 376–380.
[2] W. M. Mordey, "Electric generator," U.S. Patent 4 37 501A, Sep. 30, 1890.
[3] H. Kemper, "Schwebebahn mit raederlosen fahrzeugen, die an eisernen fahrschienen mittels magnetischer felder schwebend entlang gefuehrt werden," DE Patent 6 43 316C, Apr. 5, 1937.
[4] E. R. Laithwaite, J. F. Eastham, H. R. Bolton, and T. G. Fellows, "Linear motors with transverse flux," *Proc. Inst. Electr. Eng.*, vol. 118, no. 12, p. 1761, 1971.
[5] E. R. Laithwaite, "Linear motors with transverse flux," *Electron. Power*, vol. 17, no. 12, p. 493, 1971.
[6] J. F. Eastham and J. H. Alwash, "Transverse-flux tubular motors," *Proc. Inst. Electr. Eng.*, vol. 119, no. 12, p. 1709, 1972.
[7] P. Schwärzler, G. Bohn, and H. Schauberger, "Electromagnetic suspension and/or guide system especially for magnetically suspended vehicles," U.S. Patent US3 780 668A, Aug. 11, 1972.
[8] H. Weh and H. May, "Achievable force densities for permanent magnet excited machines in new configurations," in *Proc. Int. Conf. Electr. Mach.*, Munich, Germany, Sep. 1986, pp. 1107–1111.

[9] H. Weh and J. Jiang, "Berechnungsgrundlagen für Transversalfluß-maschinen," *Elect. Eng.*, vol. 71, no. 3, pp. 187–198, 1988.
[10] H. Weh, "Permanentmagneterregte synchronmaschinen hoher Kraft-dichte nach dem transversalflußkonzept," *etzArchiv*, vol. 10, no. 5, pp. 143–149, 1988.
[11] H. Weh and J. Landrath, "New permanent magnet excited synchronous machine with high efficiency at low speeds," in *Proc. ICEM*, 1988, pp. 35–40.
[12] H. Weh, "Multiple track transversal flux machine with ring coils—Has stator and rotor formed from several track-wise identical units to allow high rotor speed and/or large diameter," DE Patent DE4 300 440 A1, Jan. 27, 1994.
[13] A. J. Mitcham, "Transverse flux motors for electric propulsion of ships," in *Proc. IEE Colloq. New Topologies Permanent Magnet Mach.*, Jun. 1997, p. 3.
[14] E. Padurariu, L. E. Somesan, I.-A. Viorel, and L. Szabo, "Large power permanent magnet transverse flux motor, steady-state and dynamic behavior," in *Proc. ELEKTRO*, May 2012, pp. 221–224.
[15] A. Darabi, A. Sarreshtehdari, and H. Tahanian, "Design of the forced water cooling system for a claw pole transverse flux permanent magnet synchronous motor," in *Proc. 21st Iranian Conf. Electr. Eng. (ICEE)*, May 2013, pp. 1–5.
[16] K. Sato, J.-S. Shin, T. Koseki, and Y. Aoyama, "Basic experiments for high-torque, low-speed permanent magnet synchronous motor and a technique for reducing cogging torque," in *Proc. 19th Int. Conf. Electr. Mach. (ICEM)*, Sep. 2010, pp. 1–6.
[17] N. J. Baker and S. Jordan, "Comparison of two transverse flux machines for an aerospace application," *IEEE Trans. Ind. Appl.*, vol. 54, no. 6, pp. 5783–5790, Jun. 2018.
[18] S. Jordan and N. J. Baker, "Design and build of a mass critical, air-cooled transverse flux machine for aerospace," in *Proc. 22nd Int. Conf. Electr. Mach. (ICEM)*, Sep. 2016, pp. 1453–1458.
[19] M. C. Kulan, N. J. Baker, and S. Turvey, "Manufacturing challenges of a modular transverse flux alternator for aerospace," *Energies*, vol. 13, no. 16, p. 4275, Aug. 2020.
[20] R. M H, V. Murali, S. A. Vt, and C. Joseph, "A comprehensive study on transverse flux motor for direct drive low-speed spacecraft applications," *IEEE Trans. Ind. Electron.*, vol. 68, no. 1, pp. 412–422, Jan. 2021.
[21] W. Hackmann and A. Binder, "Außenläufer-transversalflussmaschinen für radnabenantriebe in straßenbahnen," ETG-Tagung, Technische Univ. Darmstadt, Darmstadt, Germany, Tech. Rep., Oct. 2004.
[22] A. Lange, "Transversalflussmaschine zum einsatz in einem direktantrieb für Fahrzeuge, insbesondere bahnantrieb," DE Patent DE19 522 382C1, Jun. 23, 1995.
[23] D.-H. Kang, Y. H. Chun, and H. Weh, "Analysis and optimal design of transverse flux linear motor with PM excitation for railway traction," *IEEE Trans. Magn.*, vol. 150, no. 4, pp. 493–499, Jul. 2003.
[24] A. Elantably and A. Masmoudi, "An approach to sizing high power density TFPM intended for hybrid bus electric propulsion," *Electric Mach. Power Syst.*, vol. 28, no. 4, pp. 341–354, Apr. 2000.
[25] A. Lange, "Motor with tranverse flux," Patent EP0 712 199 (A1), May 15, 1996.
[26] P.-E. Nordström, "Innovatives hybridbus-konzept von scania verbessert die kraftstoffeffizienz um 25 %," Mai, Press Release P09601DE, Tech. Rep., 2009.
[27] J. Bruckner, "Parallel and serial hybrid systems for citybus applications: Components and first experiences," Voith Turbo, Hong Kong, Tech. Rep., Apr. 2009.
[28] *Voith ElvoDrive*, Voith Turbo GmbH & Co. KG.
[29] B. Wüst, "ElvoDrive—Serielle dieselhybridbusse: Schlussbericht Förderkennzeichen: 03EM0017," Heidenheim, Germany, Tech. Rep., 2008.
[30] C. Pompermaier, L. Sjoberg, and G. Nord, "Design and optimization of a permanent magnet transverse flux machine," in *Proc. 20th Int. Conf. Electr. Mach.*, Sep. 2012, pp. 606–611.
[31] C. Pompermaier, J. G. Washington, L. Sjöberg, and N. Ahmed, "Reduction of cogging torque in transverse flux machines by stator and rotor pole shaping," in *Proc. IEEE Energy Convers. Congr. Expo. (ECCE)*, Sep. 2016, pp. 1–7.
[32] A. Lang, "Small but mighty: How compact TFM e-motors deliver in performance," GKN Sinter Metals Eng. GmbH, Radevormwald, Germany, Tech. Rep., Jun. 2020.
[33] N. Parspour, "Novel drive for use in electrical vehicles," in *Proc. IEEE 61st Veh. Technol. Conf.*, May 2005, pp. 2930–2933.
[34] N. J. Baker, G. J. Atkinson, J. G. Washington, B. C. Mecrow, G. L. Nord, and L. Sjöberg, "Design of high torque traction motors for automotive applications using modulated pole SMC machines," in *Proc. 6th IET Int. Conf. Power Electron., Mach. Drives (PEMD)*, Mar. 2012, pp. 27–29.
[35] A. Kleimaier and B. Hoffmann, "Axial flux motor DYNAX—A compact electric drive for automotive power trains," in *Proc. 1st Int. Electr. Drives Prod. Conf.*, Sep. 2011, pp. 1–4.
[36] A. Schoppa and P. Delarbre, "Soft magnetic powder composites and potential applications in modern electric machines and devices," *IEEE Trans. Magn.*, vol. 50, no. 4, pp. 1–4, Apr. 2014.
[37] A. Schoppa and J. Sontheim, "Weichmagnetische pulverwerkstoffe," *Elektrische Maschinen*, nos. 11, pp. 16–21, Dec. 2013.
[38] P. Seibold, M. Gartner, F. Schuller, and N. Parspour, "Design of a transverse flux permanent magnet excited machine as a near-wheel motor for the use in electric vehicles," in *Proc. 20th Int. Conf. Electr. Mach.*, Piscataway, NJ, USA, Sep. 2012, pp. 2641–2646.
[39] P. Seibold, F. Schuller, M. Beez, and N. Parspour, "Design and measurement of a laminated permanent magnet excited transverse flux machine for electrical vehicles," in *Proc. 4th Int. Electr. Drives Prod. Conf. (EDPC)*, Sep. 2014, pp. 1–6.
[40] M. Gartner, P. Seibold, and N. Parspour, "Laminated circumferential transverse flux machines–lamination concept and applicability to electrical vehicles," in *Proc. IEEE Int. Electr. Mach. Drives Conf. (IEMDC)*, May 2011, pp. 831–837.
[41] Z. Wan, A. Ahmed, I. Husain, and E. Muljadi, "A novel transverse flux machine for vehicle traction aplications," in *Proc. IEEE Power Energy Soc. Gen. Meeting*, Jul. 2015, pp. 1–5.
[42] C. Müller, B. Kalkmann, and J. Sontheim, "A highly innovated transversal flux motor design with integrated inverter," in *Proc. 2nd Int. Electric Drives Prod. Conf. (EDPC)*, Oct. 2012, pp. 1–6.
[43] U. Mühlberger, A. Lange, and R. Müller, "Use of a transversal flux machine to drive a wheel in a vehicle, and wheel drive for a vehicle," EP Patent EP0 858 149 (A1), Aug. 8, 1998.
[44] E. Schmidt, D. Brunnschweiler, and S. Berchten, "Finite element analysis of a transverse flux machine with an external rotor for wheel hub drives," in *Proc. 15th Int. Conf. Electr. Mach. (ICEM)*, Sep. 2010, pp. 1–6.
[45] Z. Jia, H. Lin, H. Yang, Z. Jia, and C. Mi, "Transverse flux permanent magnet motor with double-C stator hoops and flux-concentrated rotor for in-wheel drive electric vehicle," in *Proc. IEEE Energy Convers. Congr. Expo. (ECCE)*, Sep. 2014, pp. 4804–4808.
[46] S. Baserrah, K. Rixen, and B. Orlik, "Transverse flux machines with distributed windings for in-wheel applications," in *Proc. Int. Conf. Power Electron. Drive Syst. (PEDS)*, Nov. 2009, pp. 102–108.
[47] Z. Rahman, "Evaluating radial, axial and transverse flux topologies for 'in-wheel' motor," in *Proc. Power Electron. Transp.*, Oct. 2004, pp. 75–81.
[48] I. Martinez-Ocaña, N. J. Baker, B. C. Mecrow, C. Hilton, and S. Brockway, "Transverse flux machines as an alternative to radial flux machines in an in-wheel motor," *J. Eng.*, vol. 2019, no. 17, pp. 3624–3628, Jun. 2019.
[49] D. Takizawa, T. Takahashi, H. Shimizu, and R. Kato, "Development of transverse flux motor with improved material and manufacturing method," *SAE Int. J. Passenger Cars Electron. Electr. Syst.*, vol. 6, no. 1, pp. 366–376, Apr. 2013.
[50] L. Löwenstein, *Kurbelwellen-Starter-Generatoren Auf Der Basis Von Reluktanzmaschinen* (Berichte aus der Elektrotechnik). Aachen, Germany: Shaker, 2003.
[51] G. Q. Bao, K. F. Mao, and C. Xu, "An intelligent maximum power control for transverse flux permanent magnet generator," in *Proc. Asia–Pacific Power Energy Eng. Conf.*, 2010, pp. 1–5.
[52] D.-J. Bang, H. Polinder, G. Shrestha, and J. A. Ferreira, "Promising direct-drive generator system for large wind turbines," in *Proc. Wind Power to Grid EPE Wind Energy Chapter 1st Seminar*, Sep. 2008, pp. 1–10.
[53] D.-J. Bang, H. Polinder, G. Shrestha, and J. A. Ferreira, "Review of generator systems for direct-drive wind turbines," in *Proc. Eur. Wind Energy Conf. (EWEC)*, Brussels, Belgium, 2008, pp. 1–11.
[54] D.-j. Bang, H. Polinder, G. Shrestha, and J. A. Ferreira, "Comparative design of radial and transverse flux PM generators for direct-drive wind turbines," in *Proc. 18th Int. Conf. Electr. Mach.*, Sep. 2008, pp. 1–6.

[55] D.-J. Bang, H. Polinder, G. Shrestha, and J. A. Ferreira, "Design of a lightweight transverse flux permanent magnet machine for direct-drive wind turbines," in *Proc. IEEE Ind. Appl. Soc. Annu. Meeting*, Oct. 2008, pp. 1–7.

[56] D.-J. Bang, H. Polinder, G. Shrestha, and J. A. Ferreira, "Ring-shaped transverse flux PM generator for large direct-drive wind turbines," in *Proc. Int. Conf. Power Electron. Drive Syst. (PEDS)*, Nov. 2009, pp. 61–66.

[57] D.-J. Bang, "Design of transverse flux permanent magnet machines for large direct-drive wind turbines," Ridderprint B.V., Technische Univ. Delft, Delft, The Netherlands, Tech. Rep., 2010.

[58] A.-C. Viorel, L. Strete, and I.-A. Viorel, "Transverse flux generators a solution for stand-alone wind mill," in *Proc. 13th Int. Conf. Eng. Modern Electric Syst. (EMES)*, Jun. 2015, pp. 1–4.

[59] F. T. V. Nica, E. Ritchie, and K. Leban, "A comparison between two optimized TFPM geometries for 5 MW direct-drive wind turbines," in *Proc. 8TH Int. Symp. Adv. TOPICS Electr. Eng. (ATEE)*, May 2013, pp. 1–6.

[60] H. Groke, J. Schüttler, J. Adler, and B. Orlik, "Optimized power-feedback with an 8.7 kNm-transverse flux generator," in *Proc. 15th Int. Conf. Electr. Mach. (ICEM)*, Sep. 2010, pp. 1–6.

[61] M. B. C. Salles, J. R. Cardoso, and K. Hameyer, "Dynamic modeling of transverse flux permanent magnet generator for wind turbines," *J. Microw., Optoelectronics Electromagn. Appl.*, vol. 10, no. 1, pp. 95–105, Jun. 2011.

[62] J. Schüttler, H. Groke, M. Siatkowski, J. Adler, and B. Orlik, "Power-optimized symmetrizing current control with a 8.7 kNm-transverse flux generator," in *Proc. 12th Int. Conf. Optim. Electr. Electron. Equip.*, May 2010, pp. 352–357.

[63] D. Svechkarenko, J. Soulard, and C. Sadarangani, "A novel transverse flux generator in direct-driven wind turbines," in *Proc. ICEM*, 2006.

[64] D. Svechkarenko, *On Analytical Modeling and Design of a Novel Transverse Flux Generator for Offshore Wind Turbines* (TRITA-EE. Stockholm: Skolan för Elektro-och Systemteknik) Stockholm, Sweden: Kungliga Tekniska Högskolan, 2007, p. 021.

[65] M. R. Quddes, M. Sekino, H. Ohsaki, N. Kashima, and S. Nagaya, "Electromagnetic design study of transverse flux enhanced type superconducting wind turbine generators," *IEEE Trans. Appl. Supercond.*, vol. 21, no. 3, pp. 1101–1104, Jun. 2011.

[66] M. R. Dubois, "Optimized permanent magnet generator topologies for direct-drive wind turbines," Ph.D. dissertation, Technische Universiteit Delft, Delft, The Netherlands, 2004.

[67] A. M. Ajamloo, A. Ghaheri, and R. Nasiri-Zarandi, "Design and optimization of a new TFPM generator with improved torque profile," in *Proc. Int. Power Syst. Conf. (PSC)*, Dec. 2019, pp. 106–112.

[68] R. Nasiri-Zarandi, A. M. Ajamloo, and K. Abbaszadeh, "Proposing the output equations and 3-D MEC modeling for u -Core TFPM generators," in *Proc. Int. Symp. Power Electron., Electr. Drives, Automat. Motion (SPEEDAM)*, Jun. 2018, pp. 292–297.

[69] M. Bellucci, V. I. Cimino, and R. Rizzo, "A transverse flux permanent magnet machine for micro-wind generation application," in *Proc. Int. Conf. Clean Electr. Power (ICCEP)*, Jun. 2011, pp. 802–806.

[70] M. Rüter and W. Oberschlep, "Wirkungsgradoptimierter Direktantrieb," *A D-Kompendium*, vol. 13, pp. 58–60, 2011.

[71] M. A. Hernandez-Rodriguez, R. Iracheta-Cortez, N. Flores-Guzman, E. Hernandez-Mayoral, R. Gomez-Torres, and W. Durante-Gomez, "Designing a transverse flux PMSG with analytical methods for applications in wind turbines," in *Proc. IEEE 38th Central Amer. Panama Conv. (CONCAPAN XXXVIII)*, Nov. 2018, pp. 1–9.

[72] G. Peng, J. Wei, Y. Shi, Z. Shao, and L. Jian, "A novel transverse flux permanent magnet disk wind power generator with H-shaped stator cores," *Energies*, vol. 11, no. 4, p. 810, Mar. 2018.

[73] H. Polinder, B. C. Mecrow, A. G. Jack, P. Dickinson, and M. A. Mueller, "Conventional and TFPM linear generators for direct-drive wave energy conversion," *IEEE Trans. Energy Convers.*, vol. 20, no. 2, pp. 260–267, Jun. 2005.

[74] M. A. Mueller, "Electrical generators for direct drive wave energy converters," *IEE Proc. Gener., Transmiss. Distrib.*, vol. 149, no. 4, p. 446, 2002.

[75] H. Polinder, B. C. Mecrow, A. G. Jack, P. Dickinson, and M. A. Mueller, "Linear generators for direct-drive wave energy conversion," in *Proc. IEEE Int. Electric Mach. Drives Conf. (IEMDC)*, Jun. 2003, pp. 798–804.

[76] L. Rabenstein, A. Dietz, and N. Parspour, "Design concept of a wound field transverse flux machine using soft magnetic composite claw-poles," in *Proc. 10th Int. Electr. Drives Prod. Conf. (EDPC)*, Dec. 2020, pp. 1–5.

[77] S. Hieke, M. Stamann, T. Schallschmidt, and R. Leidhold, "Entwicklung eines getriebelosen transversalflussgenerators für fluss-strom-anwendungen," Lehrstuhl für Elektrische Antriebssysteme, Magdeburg, Germany, Tech. Rep., 2016.

[78] M. F. J. Kremers, "Analytical design of a transverse flux machine," Ph.D. dissertation, Dept. Elect. Eng., Technische Universiteit Eindhoven, Eindhoven, The Netherlands, 2016.

[79] T. Schallschmidt, M. Stamann, H. Kühn, and R. Leidhold, "Teilintegrierte und direktgekoppelte generator-wasserradkombination," Magdeburg, Germany, Tech. Rep., 2017.

[80] N. Parspour, A. Babazadeh, and B. Orlik, "Transverse flux machine design for manipulating system applications," in *Proc. PCIM*, 2004, pp. 1–5.

[81] M. Keller, S. Müller, and N. Parspour, "Design of a permanent magnetic excited transverse flux machine for robotic applications," in *Proc. 22nd Int. Conf. Electr. Mach. (ICEM)*, Sep. 2016, pp. 1520–1525.

[82] M. Keller, S. Müller, and N. Parspour, "Design of a transverse flux machine as joint drive for an articulated six-axis robot arm," in *Proc. Int. Symp. Power Electron., Electr. Drives, Automat. Motion (SPEEDAM)*, Piscataway, NJ, USA, Jun. 2016, pp. 849–854.

[83] M. Keller and N. Parspour, "Experimental identification and validation of model parameters of a permanent magnetic excited transverse flux machine for robotic applications," in *Proc. 11th IEEE Int. Conf. Compat., Power Electron. Power Eng. (CPE-POWERENG)*, Piscataway, NJ, USA, 2017, pp. 352–357.

[84] J. Terfurth, M. Schmid, and N. Parspour, "Planar aligned transverse flux machine with integrated reduction gear," in *Proc. Int. Conf. Electr. Mach. (ICEM)*, Aug. 2020, pp. 714–720.

[85] R. C. Donca, D. Popa, R. Balan, V. Iancu, and M. Manic, "Design and control of a novel type of actuator for the isoglide T3R1 parallel robot," in *Proc. 3rd Int. Symp. Resilient Control Syst.*, Aug. 2010, pp. 91–94.

[86] D.-C. Popa, V. Iancu, and L. Szabo, "Linear transverse flux motor for conveyors," Dept. Elect. Mach., Tech. Univ. Cluj-Napoca, Cluj-Napoca, Romania, Tech. Rep., 2007.

[87] J. Chang, D. Kang, J. Lee, and J. Hong, "Development of transverse flux linear motor with permanent-magnet excitation for direct drive applications," *IEEE Trans. Magn.*, vol. 41, no. 5, pp. 1936–1939, May 2005.

[88] J.-H. Chang, J.-W. Kim, and D.-H. Kang, "A novel transverse flux machine for direct drive applications," in *Proc. 12th Biennial IEEE Conf. Electromagn. Field Comput.*, Apr. 2006, p. 72.

[89] J. Xie, S.-D. Zhao, and J. Li, "Research on key techniques of green mechanical press directly driven by transverse flux machine," in *Proc. IEEE Int. Conf. Mechatronics Automat.*, Aug. 2010, pp. 1381–1386.

[90] S. K. T. Lundmark and E. S. Hamdi, "Designs of claw-pole motors for industrial applications," in *Proc. 3rd IET Int. Conf. Power Electron., Mach. Drives (PEMD)*, 2006, pp. 111–115.

[91] G. Kunze and C. Stentzel, "Wachstumkern leantec antrieb: Verbundprojekt 1: Rotor und stator: Stoff- und strukturmechanische beurteilung der system-bauteile: Schlussbericht," Dresden, Germany, Tech. Rep., 2014, doi: 10.2314/GBV:835055337.

[92] F. Dreher and N. Parspour, "A novel high-speed permanent magnet claw pole transverse flux machine for use in automation," in *Proc. Int. Symp. Power Electron. Power Electron., Electr. Drives, Automat. Motion*, Piscataway, NJ, USA, Jun. 2012, pp. 1240–1245.

[93] F. Dreher, N. Parspour, and B. Hagemann, "An advanced transverse flux machine for use in automation," in *Proc. Innovative Small Drives Micro-Motor Syst. GMM/ETG Symp.*, 2013, pp. 1–5.

[94] B. Orlik, H. Weh, U. Werner, M. Vinogradski, and W. Niemann, "Transversalfluss-direktantriebe für servo-applikationen: Abschlussbericht zum AiF-forschungsvorhaben 87-ZN," Deutsche Forschungsvereinigung für Mess-, Regelungs- und Systemtechnik e.V., Bremen, Germany, Tech. Rep., 2005.

[95] B. C. Mecrow, "High torque machines for power hand tool applications," in *Proc. Int. Conf. Power Electron. Mach. Drives*, 2002, pp. 644–649.

[96] N. Ahmed, G. J. Atkinson, N. J. Baker, L. Sjöberg, and N. Stannard, "Flux switching modulated pole machine topologies which offer greater mechanical simplicity," in *Proc. Int. Electr. Mach. Drives Conf.*, May 2013, pp. 354–358.

[97] J. G. Washington, G. J. Atkinson, N. J. Baker, A. G. Jack, B. C. Mecrow, B. B. Jensen, L. Pennander, G. L. Nord, and L. Sjöberg, "Three-phase modulated pole machine topologies utilizing mutual flux paths," *IEEE Trans. Energy Convers.*, vol. 27, no. 2, pp. 507–515, Jun. 2012.

[98] J. G. Washington, G. J. Atkinson, N. J. Baker, A. G. Jack, B. C. Mecrow, B. B. Jensen, L. Pennander, G. Nord, and L. Sjoberg, "An improved torque density modulated pole machine for low speed high torque applications," in *Proc. 6th IET Int. Conf. Power Electron., Mach. Drives (PEMD)*, 2012, pp. 27–29.
[99] S. Jordan, N. J. Baker, J. G. Washington, G. J. Atkinson, and E. Pinguey, "Construction methods for modulated pole machines," in *Proc. IEEE Int. Electr. Mach. Drives Conf. (IEMDC)*, May 2017, pp. 1–8.
[100] E. Pinguey, "On the design and construction of modulated pole machines," Ph.D. dissertation, Univ. Newcastle, Newcastle, U.K., Dec. 2010.
[101] J. G. Washington, N. Ahmed, N. J. Baker, and G. J. Atkinson, "Reduction of cogging torque and torque ripple in modulated pole machines by geometrical changes," in *Proc. 7th IET Int. Conf. Power Electron., Mach. Drives (PEMD)*, Apr. 2014, pp. 2.8.04–2.8.04.
[102] J. G. Washington, G. J. Atkinson, N. J. Baker, and L. Sjöberg, "Reduction of cogging torque and back EMF harmonics in modulated pole machine by variations in Tooth span," in *Proc. IEEE Int. Electr. Mach. Drives Conf. (IEMDC)*, May 2015, pp. 482–488.
[103] J. G. Washington, G. J. Atkinson, and N. J. Baker, "Reduction of cogging torque and EMF harmonics in modulated pole machines," *IEEE Trans. Energy Convers.*, vol. 31, no. 2, pp. 759–768, Jun. 2016.
[104] G. J. Atkinson and J. G. Washington, "Flux switching modulated pole machine," WO Patent WO2 014 161 744 (A2), Oct. 9, 2014.
[105] M. R. Harris, "Comparison of alternative topologies for VRPM (transverse-flux) electrical machines," in *Proc. IEE Colloq. New Topologies Permanent Magnet Mach.*, Jun. 1997, p. 2.
[106] T. Husain, I. Hasan, Y. Sozer, I. Husain, and E. Muljadi, "A comprehensive review of permanent magnet transverse flux machines for direct drive applications," in *Proc. IEEE Energy Convers. Congr. Expo. (ECCE)*, Oct. 2017, pp. 1255–1262.
[107] B. Zhang, "Soft magnetic composites in novel designs of electrical traction machines," Ph.D. dissertation, KIT Sci. Publishing, Karlsruhe, Germany, 2017, doi: 10.5445/KSP/1000064348.
[108] A. Argeseanu, E. Ritchie, and K. Leban, "Optimal design of the transverse flux machine using a fitted genetic algorithm with real parameters," in *Proc. 13th Int. Conf. Optim. Electr. Electron. Equip. (OPTIM)*, May 2012, pp. 671–678.
[109] R. Kruse, G. Pfaff, and C. Pfeiffer, "Transverse flux reluctance motor for direct servodrive applications," in *Proc. Conf. Rec. IEEE Ind. Appl. Conference. 33rd IAS Annu. Meeting*, Oct. 1998, pp. 655–662.
[110] H. M. Amreiz, "Difficulties and complexities encountered in the design of transverse flux machines," in *Proc. Electr. Syst. Aircr., Railway Ship Propuls.*, Oct. 2012, pp. 1–6.
[111] H. M. Amreiz, "Switched reluctance machines with simple hoop windings," in *Proc. Int. Conf. Power Electron. Mach. Drives*, Apr. 2002, pp. 522–527.
[112] J. Borecki, H. Groke, B. Orlik, and M. Joost, "Current waveform optimization for ripple-free output torque of transverse flux reluctance machines," in *Proc. Int. Aegean Conf. Electr. Mach. Power Electron. (ACEMP) Int. Conf. Optim. Elect. Electron. Equipment (OPTIM) Int. Symp. Adv. Electromechanical Motion Syst. (ELECTROMOTION)*, Sep. 2015, pp. 269–273.
[113] M. Łukaniszyn, M. Kowol, and J. Kołodziej, "Optimization of a two-phase transverse flux switched reluctance motor with an outer rotor," *Arch. Electr. Eng.*, vol. 61, no. 4, pp. 567–578, Nov. 2012.
[114] V. Z. Jajtić, "Vortriebskraftoptimierung bei der elektrisch erregten transversalflußmaschine," clausthal-zellerfeld: Papierflieger," Ph.D. dissertation, Fakultät für Maschinenbau und Elektrotechnik, Braunschweig, Techn. Univ., Clausthal-Zellerfeld, Germany, 1994.
[115] J. Yan, H. Lin, Y. Huang, H. Liu, and Z.-Q. Zhu, "Magnetic field analysis of a novel flux switching transverse flux permanent magnet wind generator with 3-D FEM," in *Proc. Int. Conf. Power Electron. Drive Syst. (PEDS)*, Nov. 2009, pp. 332–335.
[116] J. Yan, H. Lin, Y. Feng, Z. Q. Zhu, P. Jin, and Y. Guo, "Cogging torque optimization of flux-switching transverse flux permanent magnet machine," *IEEE Trans. Magn.*, vol. 49, no. 5, pp. 2169–2172, May 2013.
[117] B. Kou, X. Yang, J. Luo, and Y. Zhou, "Modeling and analysis of a transverse-flux flux-reversal motor," *IEEE Trans. Energy Convers.*, vol. 31, no. 3, pp. 1121–1131, Sep. 2016.
[118] C. C. Liu, D. Y. Wang, S. P. Wang, and Y. H. Wang, "A novel flux reversal claw pole machine with soft magnetic composite cores," *IEEE Trans. Appl. Supercond.*, vol. 30, no. 4, pp. 1–5, Jun. 2020.
[119] L. Rabenstein, A. Dietz, A. Kremser, and N. Parspour, "Semi-analytical calculation of a laminated transverse flux machine," in *Proc. Int. Conf. Electr. Mach. (ICEM)*, Aug. 2020, pp. 721–727.
[120] X. Yang, B. Kou, J. Luo, Y. Zhou, and F. Xing, "Torque characteristic analysis of a transverse flux motor using a combined-type stator core," *Appl. Sci.*, vol. 6, no. 11, p. 342, Nov. 2016.
[121] B. Kou, X. Yang, J. Luo, Y. Zhou, and H. Zhang, "Comparison of torque characteristic between two transverse flux motors with passive external rotor structure," in *Proc. 20th Int. Conf. Electr. Mach. Syst. (ICEMS)*, Aug. 2017, pp. 1–4.
[122] Q. Sun, W. Zhang, and Q. Wang, "Fundamental design and analysis of a novel bipolar transverse-flux motor with stator permanent-magnet excitation," *Chinese J. Electr. Eng.*, vol. 4, no. 1, pp. 60–66, 2018.
[123] J.-H. Chang, J.-W. Kim, J.-Y. Lee, D.-H. Kang, and K. Kim, "Design procedures of transverse flux linear motor," in *Dig. 14th Biennial IEEE Conf. Electromagn. Field Comput.*, May 2010, p. 1.
[124] D. Hyun Kang, Y. Ho Jeong, and M. H. Kim, "A study on the design of transverse flux linear motor with high power density," in *Proc. ISIE. IEEE Int. Symp. Ind. Electron.*, Jun. 2001, pp. 707–711.
[125] D. H. Kang, "Increasing of thrust force in transverse flux machine by permanent-magnet screen," *IEEE Trans. Magn.*, vol. 41, no. 5, pp. 1952–1955, May 2005.
[126] Y. H. Jeong, D.-H. Kang, J.-M. Kim, and S. M. Jang, "A design of transverse flux motor with permanent magnet shield," in *Proc. IEEE Int. Symp. Ind. Electron. (ISIE)*, Jun. 2001, pp. 995–999.
[127] M. Gärtner, "Transversalflussmaschine," DE Patent DE10 2013 200 890 A1, Jan. 21, 2013.
[128] M. Siatkowski and B. Orlik, "Flux linkage in transverse flux machines with flux concentration," in *Proc. 11th Int. Conf. Optim. Electr. Electron. Equip.*, May 2008, pp. 21–26.
[129] U. Werner, J. Schüttler, and B. Orlik, "Speed and torque control of a permanent magnet excited transverse flux motor for direct servo-drive applications," in *Proc. Eur. Conf. Power Electron. Appl.*, Sep. 2005, p. 10.
[130] A. Njeh and H. Trabelsi, "Performance improvement of different topologies of claw pole TFPM based on a 3D FEA," in *Prog. Electromagn. Res. Symp. Proc.*, Casablanca, Morocco, 2011, pp. 1–5.
[131] S. Baserrah and B. Orlik, "Comparison study of permanent magnet transverse flux motors (PMTFMs) for in-wheel applications," in *Proc. Int. Conf. Power Electron. Drive Syst. (PEDS)*, Nov. 2009, pp. 96–101.
[132] T. Husain, I. Hasan, Y. Sozer, I. Husain, and E. Muljadi, "Design of a modular E-Core flux concentrating transverse flux machine," *IEEE Trans. Ind. Appl.*, vol. 54, no. 3, pp. 2115–2128, May 2018.
[133] T. Husain, I. Hasan, Y. Sozer, I. Husain, and E. Muljadi, "Cogging torque minimization in transverse flux machines," *IEEE Trans. Ind. Appl.*, vol. 55, no. 1, pp. 385–397, Jan./Feb. 2019.
[134] L. Strete, I.-A. Viorel, and A. Viorel, "On the designing procedure of a permanent magnet transverse flux generator (PMTFG) with specific topology," in *Proc. 11th Int. Conf. Optim. Electr. Electron. Equip.*, May 2008, pp. 99–104.
[135] G. Kastinger and A. Paweletz, "Unipolar transverse flux machine," WO Patent WO0 186 785 (A1), Nov. 15, 2001.
[136] G. Kastinger, "Reducing torque ripple of transverse flux machines by structural designs," in *Proc. Int. Conf. Power Electron. Mach. Drives*, Apr. 2002, pp. 320–324.
[137] G. Kastinger, "Design of a novel transverse flux machine: Robert Bosch GmbH," in *Proc. ICEM*, 2002, pp. 1–6.
[138] S. K. T. Lundmark, "Application of 3-D computation of magnetic fields to the design of claw pole motors," Ph.D. dissertation, Division of Electr. Power Eng., Dept. Energy Environ., Chalmers Univ. Technol., Gothenburg, Sweden, 2005.
[139] P. Bastawade, B. N. Chaudhari, R. T. Ugale, and A. Pramanik, "Analytical and FEA based analysis of homopolar poly-phase transverse flux machine," in *Proc. IEEE Int. Conf. Power Electron., Drives Energy Syst. (PEDES)*, Dec. 2016, pp. 1–6.
[140] I. Hasan, M. W. Uddin, and Y. Sozer, "Transverse flux machines with rotary transformer concept for wide speed operations without using permanent magnet material," in *Proc. IEEE Appl. Power Electron. Conf. Expo. (APEC)*, Mar. 2016, pp. 638–642.
[141] P. L. Jansen, L. J. Li, and R. D. Lorenz, "Analysis of competing topologies of linear induction machines for high speed material transport systems," in *Proc. IEEE Ind. Appl. Conf. 28th IAS Annu. Meeting*, Oct. 1993, pp. 274–281.

[142] Y. Nozaki, J. Baba, K. Shutoh, and E. Masada, "Improvement of transverse flux linear induction motors performances with third order harmonics current injection," *IEEE Trans. Appl. Supercond.*, vol. 14, no. 2, pp. 1846–1849, Jun. 2004.

[143] U. Schäfer and H. Neudorfer, "Multi-phase transverse flux machine," WO Patent WO1 999 048 190A1, Mar. 16, 1999.

[144] U. Schäfer and H. Neudorfer, "Multi-phase transverse flux Machine: United States patent," U.S. Patent 6 455 970 B1, Sep. 24, 2002.

[145] G. Henneberger, "Development of a new transverse flux motor," in *Proc. IEE Colloq. New Topologies Permanent Magnet Mach.*, Jun. 1997.

[146] H. Ahn, G. Jang, J. Chang, S. Chung, and D. Kang, "Reduction of the torque ripple and magnetic force of a rotatory two-phase transverse flux machine using herringbone teeth," *IEEE Trans. Magn.*, vol. 44, no. 11, pp. 4066–4069, Nov. 2008.

[147] P. Seibold, F. Schuller, N. Parspour, and M. Gärtner, "Transversalflussmaschine in dieselelektrischem Antriebssystem," *ATZoffhighway*, vol. 5, no. 2, pp. 68–77, 2012. [Online]. Available: https://link.springer.com/article/10.1365/s35746-012-0047-x?noAccess=true

[148] P. Seibold and N. Parspour, "Analytical computation method of transverse flux permanent magnet excited machines via nodal analysis," in *Proc. Int. Conf. Electr. Mach. (ICEM)*, Piscataway, NJ, USA, Sep. 2014, pp. 410–415.

[149] W. M. Arshad, T. Backstrom, and C. Sadarangani, "Analytical design and analysis procedure for a transverse flux machine," in *Proc. IEEE Int. Electr. Mach. Drives Conf. (IEMDC)*, Jun. 2001, pp. 115–121.

[150] M. A. Patel and S. C. Vora, "Analysis of a fall-back transverse-flux permanent-magnet generator," *IEEE Trans. Magn.*, vol. 53, no. 11, pp. 1–5, Nov. 2017.

[151] M. V. F. da Luz, P. Dular, N. Sadowski, R. Carlson, and J. P. A. Bastos, "Development of analytical equations to calculate the cogging torque in transverse flux machines," in *Proc. IEEE Int. Electric Mach. Drives Conf.*, May 2009, pp. 1612–1616.

[152] S. Huang, J. Luo, and T. A. Lipo, "Analysis and evaluation of the transverse flux circumferential current machine," in *Proc. IEEE Ind. Appl. Conf. 32nd IAS Annu. Meeting*, Oct. 1997, pp. 378–384.

[153] A. Ahmed, Z. Wan, and I. Husain, "Permanent magnet transverse flux machine with overlapping stator poles," in *Proc. IEEE Energy Convers. Congr. Expo. (ECCE)*, Sep. 2015, pp. 791–798.

[154] A. Ahmed and I. Husain, "Power factor improvement of a transverse flux machine with high torque density," in *Proc. IEEE Int. Electr. Mach. Drives Conf. (IEMDC)*, May 2017, pp. 1–6.

[155] G. Yang, D. Cheng, H. Zhang, and B. Kou, "Bidirectional cross-linking transverse flux permanent magnet synchronous motor," *IEEE Trans. Magn.*, vol. 49, no. 3, pp. 1242–1248, Mar. 2013.

[156] O. Dobzhanskyi, R. Gouws, and E. Amiri, "On the role of magnetic shunts for increasing performance of transverse flux machines," *IEEE Trans. Magn.*, vol. 53, no. 2, pp. 1–8, Feb. 2017.

[157] R. Nasiri-Zarandi, A. Ghaheri, and K. Abbaszadeh, "Thermal modeling and analysis of a novel transverse flux HAPM generator for small-scale wind turbine application," *IEEE Trans. Energy Convers.*, vol. 35, no. 1, pp. 445–453, Mar. 2020.

[158] D. Svechkarenko, J. Soulard, and C. Sadarangani, "Parametric study of a transverse flux wind generator at no-load using three-dimensional finite element analysis," in *Proc. Int. Conf. Electr. Mach. Syst.*, Nov. 2009, pp. 1–6.

[159] J. F. Gieras, "Performance characteristics of a transverse flux generator," in *Proc. IEEE Int. Conf. Electric Mach. Drives*, May 2005, pp. 1293–1299.

[160] O. Dobzhanskyi, R. Gouws, and E. Amiri, "Comparison analysis of PM transverse flux outer rotor machines with and without magnetic shunts," in *Proc. IEEE Energy Convers. Congr. Expo. (ECCE)*, Sep. 2016, pp. 1–8.

[161] M. R. Harris, "Electric motors with heteropolar permanent magnets and homopolar windings: Computational study of performance limits," in *Proc. 7th Int. Conf. Electr. Mach. Drives*, 1995, pp. 237–241.

[162] S. M. Husband and C. G. Hodge, "The Rolls-Royce transverse flux motor development," in *Proc. IEEE Int. Electric Mach. Drives Conf. (IEMDC)*, Jun. 2003, pp. 1435–1440.

[163] M. Siatkowski and B. Orlik, "Influence of saturation effects in a transverse flux machine," in *Proc. 13th Int. Power Electron. Motion Control Conf.*, Sep. 2008, pp. 830–836.

[164] Z. Jia, H. Lin, S. Fang, and Y. Huang, "A novel transverse flux permanent magnet generator with double C-hoop stator and flux-concentrated rotor," *IEEE Trans. Magn.*, vol. 51, no. 11, pp. 1–4, Nov. 2015.

[165] Z. Jia and H. Lin, "Cogging torque optimization of a novel transverse flux permanent magnet generator with double C-hoop stator for wind power application," in *Proc. IEEE Magn. Conf. (INTERMAG)*, May 2015, p. 1.

[166] Z. Jia, H. Lin, S. Fang, and Y. Huang, "Cogging torque optimization of novel transverse flux permanent magnet generator with double C-hoop stator," *IEEE Trans. Magn.*, vol. 51, no. 11, pp. 1–4, Jul. 2015.

[167] Z. Jia, W. Chen, L. Huang, L. Yu, H. Jia, and J. Yang, "Comparison study on double-C stator-hoop transverse flux permanent magnet generator considering pole-pair number," in *Proc. 18th Int. Conf. Electr. Mach. Syst. (ICEMS)*, Oct. 2015, pp. 977–980.

[168] U. Khaled, R. Meer, and A. Beroual, "A novel design of three-phase transverse flux linear motor to minimize force ripples," *Arabian J. Sci. Eng.*, vol. 43, no. 6, pp. 2853–2858, Jun. 2018.

[169] P. Anpalahan, J. Soulard, and H.-P. Nee, "Design steps towards a high power factor transverse flux machine," in *Proc. Eur. Conf. Power Electron. Appl.*, 2001, pp. 1–6.

[170] M. Keller, *Entwurf Einer Permanentmagnetisch Erregten Transversalflussmaschine aus Pulververbundwerkstoff für Robotikanwendungen* (Berichte aus dem Institut für Elektrische Energiewandlung), vol. 8, 1st ed. Düren, Germany: Shaker, 2019.

[171] F. Dreher, "Entwurfs- und optimierungsprozesse für torque-antriebe mit transversaler flussführung," Ph.D. dissertation, Inst. Elect. Energy Convers., Universität Stuttgart, Stuttgart, Germany, 2015.

[172] F. Dreher, A. Ebrahimi, and N. Parspour, "Optimizing the control behavior of transverse flux machines by the use of hybrid flux conduction," in *Proc. Int. Conf. Expo. Electr. Power Eng.*, Piscataway, NJ, USA, Oct. 2012, pp. 374–378.

[173] F. Dreher and N. Parspour, "Reducing the cogging torque of PM transverse flux machines by discrete skewing of a segmented stator," in *Proc. 20th Int. Conf. Electr. Mach.*, Piscataway, NJ, USA, Sep. 2012, pp. 454–457.

[174] A. Njeh, A. Masmoudi, and A. Elantably, "3D FEA based investigation of the cogging torque of a claw pole transverse flux permanent magnet machine," in *Proc. IEEE Int. Electric Mach. Drives Conf. (IEMDC)*, Jun. 2003, pp. 319–324.

[175] Y. G. Guo, J. G. Zhu, Z. W. Lin, and J. J. Zhong, "Measurement and modeling of core losses of soft magnetic composites under 3-D magnetic excitations in rotating motors," *IEEE Trans. Magn.*, vol. 41, no. 10, pp. 3925–3927, Oct. 2005.

[176] Y. Guo, J. Zhu, and H. Lu, "Design and analysis of a permanent magnet claw pole/transverse flux motor with SMC core," in *Proc. Int. Conf. Power Electron. Drives Syst.*, Nov. 2005, pp. 1413–1418.

[177] Y. Shen, Z. Q. Zhu, J. T. Chen, R. P. Deodhar, and A. Pride, "Analytical modeling of claw-pole stator SPM brushless machine having SMC stator core," *IEEE Trans. Magn.*, vol. 49, no. 7, pp. 3830–3833, Jul. 2013.

[178] A. Ibala, A. Masmoudi, G. J. Atkinson, and A. G. Jack, "Investigation of the leakage fluxes of SMC made magnetic circuit claw pole TFPM," in *Ecologyic Vehicles Renewable Energies*. Monaco, U.K., 2009.

[179] A. Njeh and H. Trabelsi, "New design of the claw-pole transverse flux permanent magnet machine," in *Proc. 15th Int. Multi-Conf. Syst., Signals Devices (SSD)*, Mar. 2018, pp. 1311–1316.

[180] Robert Bosch GmbH, *Generatoren für Kraftfahrzeuge*, 1st ed. Germany, Stuttgart: Technische Unterrichtung, 1974. [Online]. Available: http://d-nb.info/949079006

[181] S. Baserrah, K. Rixen, and B. Orlik, "Unbalanced magnetic forces in rotational unsymmetrical transverse flux machine," in *Proc. Int. Conf. Electr. Mach. Syst.*, 2010, pp. 963–968.

[182] S. Baserrah and B. Orlik, "Initial experimental verification of a compact permanent magnet transverse flux machine in a sector configuration," in *Proc. IEEE Int. Electr. Mach. Drives Conf. (IEMDC)*, May 2011, pp. 1159–1164.

[183] S. Baserrah and B. Orlik, "Eddy current investigation study for a non-conventional flux concentrated permanent magnet transverse flux machine using finite element method via 3D transient approach," in *Proc. IEEE Int. Electr. Mach. Drives Conf. (IEMDC)*, May 2011, pp. 47–52.

[184] S. Baserrah and B. Orlik, "Design and optimization of concentric saddle shaped coils for permanent magnet transverse flux machine in segmented construction," in *Proc. IEEE Int. Electr. Mach. Drives Conf. (IEMDC)*, May 2011, pp. 630–635.

[185] S. Baserrah, K. Rixen, and B. Orlik, "3D–transient finite element analysis of transverse flux machine for mobile platform with external circuit connection and electromechanical coupling," in *Proc. IEEE Int. Conf. Mechatronics*, Apr. 2011, pp. 585–590.

[186] S. Baserrah, K. Rixen, and B. Orlik, "Unbalanced magnetic forces in rotational unsymmetrical transverse flux machine," *J. Electr. Eng. Technol.*, vol. 7, no. 2, pp. 184–192, Mar. 2012.
[187] S. Baserrah, "Theoretical and experimental investigations of a permanent magnet excited transverse flux machine with a segmented stator for in-wheel motor applications," Ph.D. dissertation, Inst. Elect. Drives, Power Electron. Devices, IALB, Universität Bremen, Bremen, Germany, 2013.
[188] C. G. Turker and F. E. Kuyumcu, "Determining of the magnetic characteristics of the E-core transverse flux machine based on neural network," in *Proc. Int. Symp. Innov. Intell. Syst. Appl.*, Jun. 2011, pp. 217–222.
[189] A. Chowdhury, S. Das, T. Tsuda, N. Saito, S. Saha, and Y. Sozer, "Design and analysis of a high saliency transverse flux machine with a novel rotor structure for traction applications," in *Proc. IEEE Energy Convers. Congr. Exposit. (ECCE)*, Oct. 2020, pp. 1743–1748.
[190] Y. Gong, W. Zheng, D. Zhang, and J. Jiang, "Analysis of a transverse flux machine with E-shaped stator using three dimensional scalar potential finite element method," in *Proc. IEEE 6th Int. Power Electron. Motion Control Conf.*, May 2009, pp. 1991–1994.
[191] V. Zweygbergk and G. A. Svante, "Permanent magnetized synchronous machine designed according to the transverse flux principle," U.S. Patent US5 117 142A, May 26, 1992.
[192] W. M. Arshad, "Investigating a transverse flux machine with intermediate poles," in *Proc. Int. Conf. Power Electron. Mach. Drives*, Apr. 2002, pp. 325–328.
[193] I. Hasan, T. Husain, Y. Sozer, I. Husain, and E. Muljadi, "Mechanical and thermal performance of transverse flux machines," in *Proc. IEEE Energy Convers. Congr. Expo. (ECCE)*, Oct. 2017, pp. 1205–1211.
[194] I. Hasan, T. Husain, M. W. Uddin, Y. Sozer, I. Husain, and E. Muljadi, "Analytical modeling of a novel transverse flux machine for direct drive wind turbine applications," in *Proc. IEEE Energy Convers. Congr. Exposit. (ECCE)*, Sep. 2015, pp. 2161–2168.
[195] I. Hasan, A. Chowdhury, and Y. Sozer, "Effect of pole shaping on cogging torque, torque ripple and vibrational performance in consequent pole TFM," in *Proc. IEEE Energy Convers. Congr. Exposit. (ECCE)*, Sep. 2018, pp. 7330–7335.
[196] T. Husain, I. Hasan, Y. Sozer, I. Husain, and E. Muljadi, "Design considerations of a transverse flux machine for direct-drive wind turbine applications," in *Proc. IEEE Energy Convers. Congr. Exposit. (ECCE)*, Sep. 2016, pp. 1–8.
[197] J. Tanaka and K. Sakai, "Enhanced transverse-flux motor with torus coils," in *Proc. Int. Power Electron. Conf. (IPEC-Hiroshima)*, 2014, pp. 240–245.
[198] K. Sakai and J. Tanaka, "Transverse-flux motor for enhanced torque and reduction of torque ripple," in *Proc. 17th Eur. Conf. Power Electron. Appl. (EPE ECCE-Europe)*, Sep. 2015, pp. 1–10.
[199] H. Chen, R. Nie, and H. Wang, "A transverse flux single-phase tubular-switched reluctance linear launcher with eight-pole structure," *IEEE Trans. Plasma Sci.*, vol. 47, no. 5, pp. 2331–2338, May 2019.
[200] D.-C. Popa, V.-I. Gliga, L. Szabo, and V. Iancu, "Tubular transverse flux variable reluctance motor in modular construction," in *Proc. 13th Int. Conf. Optim. Electr. Electron. Equip. (OPTIM)*, May 2012, pp. 572–577.
[201] I.-A. Viorel, K. Hameyer, and L. Strete, "Transverse flux tubular switched reluctance motor," in *Proc. 11th Int. Conf. Optim. Electr. Electron. Equip.*, May 2008, pp. 131–136.
[202] S. Zhu, T. Cox, and C. Gerada, "Comparative study of novel tubular flux-reversal transverse flux permanent magnet linear machine," in *Proc. IEEE Energy Convers. Congr. Expo. (ECCE)*, Oct. 2017, pp. 4282–4287.
[203] J. Zou, M. Zhao, Q. Wang, J. Zou, and G. Wu, "Development and analysis of tubular transverse flux machine with permanent-magnet excitation," *IEEE Trans. Ind. Electron.*, vol. 59, no. 5, pp. 2198–2207, May 2012.
[204] Z. Mei, Z. Ji-bin, J. Xin-tong, X. Fu, and C. Sadarangani, "Influence of axial length ratio of stator segment on performance of tubular transverse flux linear machine," in *Dig. 14th Biennial IEEE Conf. Electromagn. Field Comput.*, May 2010, p. 1.
[205] J. F. Pan, N. C. Cheung, and Y. Zou, "Design and analysis of a novel transverse-flux tubular linear machine with gear-shaped teeth structure," *IEEE Trans. Magn.*, vol. 48, no. 11, pp. 3339–3343, Nov. 2012.
[206] D.-C. Popa, D. D. Micu, O.-R. Miron, and L. Szabo, "Optimized design of a novel modular tubular transverse flux reluctance machine," *IEEE Trans. Magn.*, vol. 49, no. 11, pp. 5533–5542, Nov. 2013.
[207] Q. Wang, J. Zou, J. Zou, and M. Zhao, "Analysis and computer-aided simulation of cogging force characteristic of a linear electromagnetic launcher with tubular transverse flux machine," *IEEE Trans. Plasma Sci.*, vol. 39, no. 1, pp. 157–161, Jan. 2011.
[208] M. Zhao, J.-M. Zou, Y.-X. Xu, J.-B. Zou, and Q. Wang, "The thrust characteristic investigation of transverse flux tubular linear machine for electromagnetic launcher," *IEEE Trans. Plasma Sci.*, vol. 39, no. 3, pp. 925–930, Mar. 2011.
[209] J. Zou, Q. Wang, and Y. Xu, "Influence of the permanent magnet magnetization length on the performance of a tubular transverse flux permanent magnet linear machine used for electromagnetic launch," *IEEE Trans. Plasma Sci.*, vol. 39, no. 1, pp. 241–246, Jan. 2011.
[210] J.-H. Chang, J.-Y. Lee, J.-W. Kim, S.-U. Chung, D.-H. Kang, and H. Weh, "Development of rotating type transverse flux machine," in *Proc. IEEE Int. Electr. Mach. Drives Conf.*, May 2007, pp. 1090–1095.
[211] J.-Y. Lee, J.-H. Chang, D.-H. Kang, S.-I. Kim, and J.-P. Hong, "Tooth shape optimization for cogging torque reduction of transverse flux rotary motor using design of experiment and response surface methodology," *IEEE Trans. Magn.*, vol. 43, no. 4, pp. 1817–1820, Apr. 2007.
[212] T. Schallschmidt, M. Stamann, H. Kühn, and R. Leidhold. (Sep. 2017). *Teilintegrierte und Direktgekoppelte Generator-Wasserradkombination*. 13. Magdeburger Maschinenbau-Tage 2017: Autonom—Vernetzt—Nachhaltig. Tagungsband. Magdeburg: Universitätsbibliothek. [Online]. Available: http://nbn-resolving.de/urn: nbn: de: gbv: ma9:1-10182
[213] U. Werner, *Optimierung der Betriebseigenschaften permanenterregter Transversalflussmaschinen als Servo-Direktantriebe* (Berichte des Instituts für elektrische Antriebe Leistungselektronik und Bauelemente der Universität Bremen), vol. 382. Düsseldorf, Germany: VDI-Verl., 2008.
[214] U. Werner, "Optimization of the operation behaviour of a permanent magnet excited transverse flux motor for direct servo-drive applications," *Sci. J. Gdynia Maritime Univ.*, no. 101, pp. 53–63, 2017. [Online]. Available: http://zeszyty.am.gdynia.pl/artykul-2518.html
[215] B. Zhang, T. Epskamp, M. Doppelbauer, and M. Gregor, "A comparison of the transverse, axial and radial flux PM synchronous motors for electric vehicle," in *Proc. IEEE Int. Electr. Vehicle Conf. (IEVC)*, Dec. 2014, pp. 1–6.
[216] M. Waldhof, A. Echle, and N. Parspour, "A novel drive train concept for personalized upper body exoskeletons with a multiphase axial flux machine," in *Proc. IEEE Int. Electr. Mach. Drives Conf. (IEMDC)*, May 2019, pp. 2160–2166.
[217] R. Blissenbach and I.-A. Viorel, "On the single-sided transverse flux machine design," *Electr. Power Compon. Syst.*, vol. 31, no. 2, pp. 109–128, Feb. 2003.
[218] J. G. Washington, C. Pompermaier, and G. J. Atkinson, "Robust electromagnetic design of transverse flux machines for high volume production," in *Proc. 32nd Int. Conf. Electr. Mach. (ICEM)*, Sep. 2016, pp. 877–883.
[219] J. Doering, G. Steinborn, and W. Hofmann, "Torque, power, losses, and heat calculation of a transverse flux reluctance machine with soft magnetic composite materials and disk-shaped rotor," *IEEE Trans. Ind. Appl.*, vol. 51, no. 2, pp. 1494–1504, Mar./Apr. 2015.
[220] J. Schüttler and B. Orlik, "Analytical model describing the operation behaviour of transverse flux machines in flat magnet configuration," in *Proc. Eur. Conf. Power Electron. Appl.*, Sep. 2007, pp. 1–10.
[221] N. Götschmann, "High torque generators in weigth saving construction: Hochmoment-generatoren in leichtbauweise," Energy 2.0, Tech. Rep. E2118451, Nov. 2008, pp. 42–44.
[222] M. R. Harris, "The problem of power factor in VRPM (transverse-flux) machines," in *Proc. 8th Int. Conf. Electr. Mach. Drives*, Sep. 1997, pp. 386–390.
[223] Y. G. Guo, J. G. Zhu, P. A. Watterson, and W. Wu, "Development of a PM transverse flux motor with soft magnetic composite core," *IEEE Trans. Energy Convers.*, vol. 21, no. 2, pp. 426–434, Jun. 2006.
[224] J. D. Lee, D. K. Hong, B. C. Woo, D. H. Park, and B. U. Nam, "Performance comparison of longitudinal flux and transverse flux permanent magnet machines for turret applications with large diameter," *IEEE Trans. Magn.*, vol. 48, no. 2, pp. 915–918, Feb. 2012.
[225] A. Chen, R. Nilssen, and A. Nysveen, "Performance comparisons among radial-flux, multistage axial-flux, and three-phase transverse-flux PM machines for downhole applications," *IEEE Trans. Ind. Appl.*, vol. 46, no. 2, pp. 779–789, Jan. 2010.

[226] J. Pippuri, A. Manninen, J. Keranen, and K. Tammi, "Torque density of radial, axial and transverse flux permanent magnet machine topologies," *IEEE Trans. Magn.*, vol. 49, no. 5, pp. 2339–2342, May 2013.

[227] J. Bauer, "Sensorlose hystereseregelung einer permanenterregten transversalflussmaschine," Ph.D. dissertation, Fakultät für Elektrotechnik und Informationstechnik, Technische Universität München, München, Germany, 2017.

[228] M. Bork, *Entwicklung und Optimierung Einer fertigungsgerechten Transversalflußmaschine*(Berichte aus der Elektrotechnik). Aachen, Germany: Shaker, 1997.

[229] R. Blissenbach, *Entwicklung von Permanenterregten Transversalfluß-maschinen Hoher Drehmomentdichte für Traktionsantriebe* (Berichte aus der Elektrotechnik). Aachen, Germany: Shaker, 2002.

[230] U. Werner, J. Schüttler, and B. Orlik, "Position control of a transverse flux motor with reduced torque ripples for direct servo-drive applications using shaped currents with harmonics control," in *Proc. Eur. Conf. Power Electron. Appl.*, Sep. 2007, pp. 1–10.

[231] *High Torque Direktantriebe TorqueChampion: Power at Work!*, Landert Motoren AG, Zürich, Switzerland, 2008.

[232] O. Schwab, "Verbundprojekt: Großserientaugliches herstellverfahren für neuartige elektrische axialflussmotoren (GroAx)," Compact Dyn. GmbH, Starnberg, Germany, Tech. Rep., 2016.

[233] P. Seibold, "Analytisches Verfahren zur berechnung einer dreisträngigen geblechten transversalflussmaschine für traktionsantriebe," Ph.D. dissertation, Inst. Elect. Energy Convers., Universität Stuttgart, Stuttgart, Germany, 2015.

[234] A. Boehm and I. Hahn, "Comparison of soft magnetic composites (SMCs) and electrical steel," in *Proc. 2nd Int. Electr. Drives Prod. Conf. (EDPC)*, Oct. 2012, pp. 1–6.

[235] N. Dehlinger and M. R. Dubois, "Clawpole transverse flux machines with amorphous stator cores," in *Proc. 18th Int. Conf. Electr. Mach.*, Sep. 2008, pp. 1–6.

[236] N. Dehlinger and M. R. Dubois, "A simple insulated thermometric method for the experimental determination of iron losses," in *Proc. 18th Int. Conf. Electr. Mach.*, Sep. 2008, pp. 1–6.

[237] S. Müller, M. Keller, A. Enssle, A. Lusiewicz, P. Präg, D. Maier, J. M. Fischer, and N. Parspour, "3D-FEM simulation of a transverse flux machine respecting nonlinear and anisotropic materials," in *Proc. Comsol Conf.*, 2016, pp. 1–6.

[238] K. Lu and W. Wu, "High torque density transverse flux machine without the need to use SMC material for 3-D flux paths," *IEEE Trans. Magn.*, vol. 51, no. 3, pp. 1–4, Mar. 2015.

[239] M. R. Dubois, H. Polinder, and J. A. Ferreira, "Prototype of a new transverse-flux permanent magnet (TFPM) machine with toothed rotor," in *Proc. Int. Conf. Electr. Mach.*, 2002, pp. 1–6.

[240] F. Schuller, M. Maier, P. Seibold, and N. Parspour, "Modeling and parameter estimation of a three phase permanent magnet excited transverse flux machine," in *Proc. 22nd Int. Conf. Electr. Mach. (ICEM)*, Sep. 2016, pp. 439–444.

[241] A. Ibala, A. Masmoudi, G. J. Atkinson, and A. G. Jack, "A new reluctance model of a claw pole TFPM using SMC for the magnetic circuit," in *Ecologic Vehicles Renewable Energies*. Monaco, U.K., 2009.

[242] A. Ibala, A. Masmoudi, G. J. Atkinson, and A. G. Jack, "On the modeling of a TFPM by reluctance network including the saturation effect with emphasis on the leakage fluxes," *COMPEL Int. J. Comput. Math. Electr. Electron. Eng.*, vol. 30, no. 1, pp. 151–171, 2011.

[243] Y. Dou, Y. Guo, and J. Zhu, "Investigation of motor topologies for SMC application," in *Proc. Int. Conf. Electr. Mach. Syst. (ICEMS)*, Oct. 2007, pp. 695–698.

[244] J. Zhu and Y. Guo, "Study with magnetic property measurement of soft magnetic composite material and its application in electrical machines," in *Proc. IEEE Ind. Appl. Conf. 39th IAS Annu. Meeting*, Oct. 2004, pp. 373–380.

[245] *Somaloy Prototyping Material, SPM: Datasheet*, Höganäs AB, 1334HOG, 2016.

[246] F. Mannerhagen, "Designing and prototyping of a transverse flux machine in soft magnetic composite using milling and turning techniques," M.S. thesis, Dept. Electr. Power Eng. Energy Environ., Chalmers Univ. Technol., Göteborg, Sweden, 2017.

[247] J.-Y. Lee, S.-R. Moon, D.-H. Koo, D.-H. Kang, G.-H. Lee, and J.-P. Hong, "Comparative study of stator core composition in transverse flux rotary machine," *J. Electr. Eng. Technol.*, vol. 6, no. 3, pp. 350–355, May 2011.

[248] N. Stannard, J. G. Washington, and G. J. Atkinson, "A comparison of axial field topologies employing SMC for traction applications," in *Proc. 19th Int. Conf. Electr. Mach. Syst. (ICEMS)*, 2016, pp. 1–6.

[249] M. Gartner, N. Parspour, and T. Burgstaller, "Hardware emulation of transverse flux machines based on an analytical model considering saturation effects," in *Proc. 19th Int. Conf. Electr. Mach. (ICEM)*, Sep. 2010, pp. 1–6.

[250] N. Götschmann and W. Hüneberg, "Enclosure for active components, in particular rotor or stator ring, for an electric machine, in particular transversal flux machine," EP Patent EP1 928 072 (A2), Jun. 4, 2008.

[251] M. Gräf, *Einseitige Transversalflußmaschine Mit Multifunktionellem, Keramischem Tragring* (Berichte aus der Elektrotechnik). Aachen, Germany: Shaker, 2001.

[252] M. Gärtner, "Modellbildung einer transversalflussmaschine für die stationäre und dynamische Simulation," Ph.D. dissertation, Inst. Elect. Energy Convers., Universität Stuttgart, Stuttgart, Germany, 2014.

[253] D.-H. Kang, J.-W. Kim, D. O. Kisck, V. Navrapescu, and M. Kisck, "Dynamic simulation of the transverse flux machine using linear model and finite element method," in *Proc. 33rd Annu. Conf. IEEE Ind. Electron. Soc. (IECON)*, Nov. 2007, pp. 1304–1309.

[254] Z. Yu and C. Jianyun, "Power factor analysis of transverse flux permanent machines," in *Proc. Int. Conf. Electr. Mach. Syst.*, Sep. 2005, pp. 450–459.

[255] P. Anpalahan, *Design of Transverse Flux Machines Using Analytical Calculations & Finite Element Analysis*. Stockholm, Sweden: Royal Institute of Technology, 2001.

[256] J. Bauer and A. Kleimaier, "Modeling a transversalflux machine representing effects relevant for sensorless control," in *Proc. Int. Conf. Electr. Mach. (ICEM)*, Sep. 2014, pp. 564–570.

[257] I. Hasan, T. Husain, Y. Sozer, I. Husain, and E. Muljadi, "Analytical model-based design optimization of a transverse flux machine," in *Proc. IEEE Energy Convers. Congr. Expo. (ECCE)*, Sep. 2016, pp. 1–7.

[258] I. Hasan, T. Husain, Y. Sozer, I. Husain, and E. Muljadi, "Analytical modeling of a double-sided flux concentrating E-Core transverse flux machine with pole windings," in *Proc. IEEE Int. Electr. Mach. Drives Conf. (IEMDC)*, May 2017, pp. 1–7.

[259] A. Ibala, R. Rebhi, and A. Masmoudi, "MEC-based modelling of claw pole machines: Application to automotive and wind generating systems," *Int. J. Renew. Energy Res.*, vol. 1, no. 3, pp. 110–117, 2011.

[260] J. F. Klöck, T. Orlik, and W. Schumacher, "Modeling and torque ripple minimization of transverse flux machines," in *Proc. 15th Eur. Conf. Power Electron. Appl. (EPE)*, Sep. 2013, pp. 1–8.

[261] M. Zafarani, M. Moallem, and A. Tabesh, "Analytical model for a transverse flux permanent magnet machine using improved magnetic equivalent circuit approach," in *Proc. 21st Int. Conf. Syst. Eng.*, Aug. 2011, pp. 96–99.

[262] N. Parspour and B. Orlik, "Design of transverse flux machines using analytical and numerical computing methods," in *Proc. 6th Int. Conf. Comput. Electromagn.*, 2006, pp. 1–2.

[263] M. Gartner, F. Schuller, N. Parspour, and P. Seibold, "Analytical modeling and simulation of highly utilized electrical machines considering nonlinear effects," in *Proc. 20th Int. Conf. Electr. Mach.*, Sep. 2012, pp. 2786–2791.

[264] M. F. J. Kremers, J. J. H. Paulides, J. L. G. Janssen, and E. A. Lomonova, "Analytical flux linkage and EMF calculation of a transverse flux machine," in *Proc. Int. Conf. Electr. Mach. (ICEM)*, Sep. 2014, pp. 2668–2673.

[265] M. F. J. Kremers, J. J. H. Paulides, J. L. G. Janssen, and E. A. Lomonova, "Analytical 3-D force calculation of a transverse flux machine," in *Proc. ELECTRIMACS*, 2014, pp. 220–225.

[266] M. F. J. Kremers, J. J. H. Paulides, and E. A. Lomonova, "Analytical 3-D design of a transverse flux machine with high power factor," in *Proc. Int. Conf. Sustain. Mobility Appl., Renewables Technol. (SMART)*, Nov. 2015, pp. 1–5.

[267] M. F. J. Kremers, J. J. H. Paulides, and E. A. Lomonova, "Toward accurate design of a transverse flux machine using an analytical 3-D magnetic charge model," *IEEE Trans. Magn.*, vol. 51, no. 11, pp. 1–4, Nov. 2015.

[268] M. Kremers, J. J. Paulides, and E. Lomonova, "Design and optimization of a transverse flux machine using an analytical 3-D magnetic charge model," in *Proc. IEEE Magn. Conf. (INTERMAG)*, May 2015, p. 1.

[269] M. F. J. Kremers, D. V. Casteren, J. J. H. Paulides, and E. A. Lomonova, "Semi-analytical 3-D magnetic charge model for force calculation of a transverse flux machine," in *Proc. 10th Int. Conf. Ecol. Vehicles Renew. Energies (EVER)*, Mar. 2015, pp. 1–7.
[270] I.-A. Viorel, A. D. Popan, L. Szabo, and R. C. Ciorba, "Direct drive system with two phase transverse flux disc-type motor," in *Proc. Int. Conf. Power Electron., Intell. Motion Power Quality (PCIM)*, Nürnberg, Germany, 2005, pp. 1–6.
[271] D. Svechkarenko, J. Soulard, and C. Sadarangani, "Performance evaluation of a novel transverse flux generator with 3D finite element analysis," in *Proc. Int. Conf. Electr. Mach. Syst.*, Nov. 2009, pp. 1–6.
[272] R. Meer, H. M. Hasanien, and A. I. Alolah, "Dynamic simulation of single phase transverse flux linear motor," in *Proc. Int. Renew. Sustain. Energy Conf. (IRSEC)*, Oct. 2014, pp. 493–498.
[273] G. Deliege, "3D finite element computation of a linear transverse flux actuator," in *Proc. Int. Conf. Power Electron. Mach. Drives*, Apr. 2002, pp. 315–319.
[274] B. E. Hasubek and E. P. Nowicki, "Two dimensional finite element analysis of passive rotor transverse flux motors with slanted rotor design," in *Proc. Eng. Solutions Next Millennium. IEEE Can. Conf. Electr. Comput. Eng.*, May 1999, pp. 1199–1204.
[275] B. E. Hasubek and E. P. Nowicki, "Design limitations of reduced magnet material passive rotor transverse flux motors investigated using 3D finite element analysis," in *Proc. IEEE Can. Conf. Elect. Comput. Eng.*, Halifax, NS, Canada, May 2000, pp. 365–369.
[276] E. Schmidt, "Finite element analysis of a novel design of a three phase transverse flux machine with an external rotor," in *Dig. 14th Biennial IEEE Conf. Electromagn. Field Comput.*, May 2010, p. 1.
[277] E. Schmidt, "Finite-elemente-analyse einer transversalflussmaschine," *Elektrotechnik Informationstechnik*, vol. 117, no. 2, pp. 124–128, Feb. 2000.
[278] E. Schmidt, "3-D finite element analysis of the cogging torque of a transverse flux machine," *IEEE Trans. Magn.*, vol. 41, no. 5, pp. 1836–1839, May 2005.
[279] E. Schmidt, D. Brunnschweiler, and S. Berchten, "Finite element analysis of a transverse flux machine with an external rotor for wheel hub drives," in *Proc. 19th Int. Conf. Electr. Mach. (ICEM)*, Sep. 2010, pp. 1–6.
[280] S. Müller, M. Siegle, M. Keller, and N. Parspour, "Loss calculation for electrical machines based on finite element analysis considering 3D magnetic flux," in *Proc. 13th Int. Conf. Electr. Mach. (ICEM)*, Sep. 2018, pp. 1246–1252.
[281] J. Schüttler and B. Orlik. (2006). *Simulation Einer Transversalflussmaschine in Flachmagnetanordnung*. NAFEMS Magazin Zeitschrift für Numerische Simulationsmethoden und angrenzende Gebiete. [Online]. Available: https://www.nafems.org/downloads/magazin/nl4 high.pdf
[282] K. Y. Lu, E. Ritchie, P. O. Rasmussen, and P. Sandholdt, "General torque equation capable of including saturation effects for a single phase surface mounted permanent magnet transverse flux machine," in *Proc. 38th IAS Annu. Meeting Conf. Rec. Ind. Appl. Conf.*, Oct. 2003, pp. 1382–1388.
[283] K. Y. Lu, E. Ritchie, P. O. Rasmussen, and P. Sandholdt, "Modeling and power factor analysis of a single phase surface mounted permanent magnet transverse flux machine," in *Proc. 5th Int. Conf. Power Electron. Drive Syst. (PEDS)*, Nov. 2003, pp. 1609–1613.
[284] M. Siatkowski, J. Schüttler, and B. Orlik, "FEM-data based model for fast simulation of a transverse flux machine," in *Proc. 19th Int. Conf. Electr. Mach. (ICEM)*, Sep. 2010, pp. 1–6.
[285] J. Y. Lee, J. W. Kim, J. H. Chang, S. U. Chung, D. H. Kang, and J. P. Hong, "Determination of parameters considering magnetic nonlinearity in solid core transverse flux linear motor for dynamic simulation," *IEEE Trans. Magn.*, vol. 44, no. 6, pp. 1566–1569, Jun. 2008.
[286] I.-A. Viorel, L. Szabo, and Z. Puklus, "Transverse flux motor drive dynamics," in *Proc. IEEE Int. Conf. Intell. Syst.*, Cluj-Napoca, Romania, 2004.
[287] H. R. Karimi, A. Babazadeh, and N. Parspour, "Robust output tracking of transverse flux machines using RBF neural network," in *Proc. IEEE Conf. Robot., Automat. Mechatronics,.*, Dec. 2004, pp. 496–501.
[288] H. R. Karimi and A. Babazadeh, "Modeling and output tracking of transverse flux permanent magnet machines using high gain observer and RBF neural network," *ISA Trans.*, vol. 44, no. 4, pp. 445–456, Oct. 2005.
[289] H. Karimi, A. Babazadeh, P. J. Maralani, B. Moshiri, and N. Parspour, "Sensorless adaptive output tracking of transverse flux permanent magnet machines," *ARI Bull. Istanbul Tech. Univ.*, vol. 54, no. 3, pp. 17–23, 2005.
[290] A. Babazadeh and H. R. Karimi, "Adaptive output tracking of transverse flux machines using neuro-fuzzy approach," *J. Appl. Sci. Eng.*, vol. 9, no. 2, pp. 115–120, 2006.
[291] A. Babazadeh, H. R. Karimi, and N. Parspour, "Robust adaptive control of transverse flux permanent magnet machines using neural networks," *IFAC Proc. Volumes*, vol. 38, no. 1, pp. 169–174, 2005.
[292] A. Babazadeh, H. R. Karimi, and B. Moshiri, "A neuro-fuzzy based approach for output tracking of transverse flux machines," in *Proc. IEEE Conf. Control Appl. (CCA)*, Aug. 2005, pp. 272–276.
[293] H. M. Hasanien, S. M. Muyeen, and J. Tamura, "Speed control of permanent magnet excitation transverse flux linear motor by using adaptive neuro-fuzzy controller," *Energy Convers. Manage.*, vol. 51, no. 12, pp. 2762–2768, Dec. 2010.
[294] A. Keyhani, C. B. Studer, T. Sebastian, and S. K. Murthy, "Study of cogging torque in permanent magnet machines," *Electric Mach. Power Syst.*, vol. 27, no. 7, pp. 665–678, Jun. 1999.
[295] Y. Ueda, H. Takahashi, A. Ogawa, T. Akiba, and M. Yoshida, "Cogging-torque reduction of transverse-flux motor by skewing stator poles," *IEEE Trans. Magn.*, vol. 52, no. 7, pp. 1–4, Jul. 2016.
[296] A. Masmoudi, A. Njeh, and A. Elantably, "On the analysis and reduction of the cogging torque of a claw pole transverse flux permanent magnet machine," *Eur. Trans. Electr. Power*, vol. 15, no. 6, pp. 513–526, 2005.
[297] R. Nasiri-Zarandi and A. M. Ajamloo, "Implementation of PM step skew technique to optimum design of a transverse flux PM generator for small scale wind turbine," in *Proc. IEEE Milan PowerTech*, Jun. 2019, pp. 1–6.
[298] Y. Ueda and H. Takahashi, "Cogging torque reduction on transverse-flux motor with multilevel skew configuration of toothed cores," *IEEE Trans. Magn.*, vol. 55, no. 7, pp. 1–5, Jul. 2019.
[299] A. Masmoudi, A. Njeh, A. Mansouri, H. Trabelsi, and A. Elantably, "Optimizing the overlap between the stator teeth of a claw pole transverse-flux permanent-magnet Machine," *IEEE Trans. Magn.*, vol. 40, no. 3, pp. 1573–1578, May 2004.
[300] C. Liu, J. Zhu, Y. Wang, and G. Lei, "Cogging torque minimization of SMC PM transverse flux machines using shifted and unequal-width stator teeth," *IEEE Trans. Magn.*, vol. 26, no. 4, pp. 1–4, Jun. 2016.
[301] J. G. Washington, C. Pompermaier, and G. J. Atkinson, "Optimisation of the torque quality of a combined phase transverse flux machine for traction applications," in *Proc. IEEE Energy Convers. Congr. Expo. (ECCE)*, Sep. 2016, pp. 1–6.
[302] F. Dreher, A. Ebrahimi, and N. Parspour, "Balancing torque loss and cogging reduction at PM transverse flux machines with segmented stator phases," in *Proc. PCIM Eur.*, 2013, pp. 105–111.
[303] J. Fischer, M. Schmid, and N. Parspour, "Investigation of maximum torque per ampere and maximum efficiency control strategies of a transverse flux machine," in *Proc. Int. Conf. Electr. Mach. (ICEM)*, Aug. 2020, pp. 2527–2532.
[304] A. Ebrahimi, F. Dreher, and N. Parspour, "Sensorless direct torque control of transverse flux machines with hybrid flux conduction," in *Proc. PCIM Eur.*, 2013, pp. 97–104.
[305] E. Favre, L. Cardoletti, and M. Jufer, "Permanent-magnet synchronous motors: A comprehensive approach to cogging torque suppression," *IEEE Trans. Ind. Appl.*, vol. 29, no. 6, pp. 1141–1149, Nov. 1993.
[306] M. Gartner, N. Parspour, P. Seibold, R. Bohl, and M. Klein, "Position control of a permanent magnet transverse flux machine with very high force density for industrial automation systems," in *Proc. 14th Int. Power Electron. Motion Control Conf. EPE-PEMC*, Piscataway, NJ, USA, Sep. 2010, p. 65.
[307] F. Schuller, N. Parspour, and L. Chen, "Position control of a linear transverse flux machine with subordinate current control," in *Proc. Int. Conf. Electr. Mach. (ICEM)*, Piscataway, NJ, USA, Sep. 2014, pp. 629–633.
[308] C. Pfeiffer, "Einsatz von Reluktanzmotoren für langsam laufende Servodirektantriebe," Ph.D. dissertation, Erlangen: Technische Fakultät der Universität Erlangen-Nürnberg, Nürnberg, Germany, 2000.
[309] Y. Xu, N. Parspour, and U. Vollmer, "Torque ripple minimization for PMSM using online estimation of the stator resistances," in *Proc. 20th Int. Conf. Electr. Mach.*, Piscataway, NJ, USA, Sep. 2012, pp. 1107–1113.

[310] M. R. Harris, G. H. Pajooman, and S. M. Abu Sharkh, "Performance and design optimisation of electric motors with heteropolar surface magnets and homopolar windings," *IEE Proc. - Electric Power Appl.*, vol. 143, no. 6, p. 429, 1996.
[311] A. Ahmed and I. Husain, "Power factor improvement of a transverse flux machine with high torque density," *IEEE Trans. Ind. Appl.*, vol. 54, no. 5, pp. 4297–4305, Sep. 2018.
[312] K. Lu, P. O. Rasmussen, and E. Ritchie, "Design considerations of permanent magnet transverse flux machines," *IEEE Trans. Magn.*, vol. 47, no. 10, pp. 2804–2807, Oct. 2011.
[313] J. R. Anglada and S. M. A. Sharkh, "An insight into torque production and power factor in transverse-flux machines," in *Proc. 32nd Int. Conf. Electr. Mach. (ICEM)*, Feb. 2016, pp. 120–125.
[314] G. Patterson, T. Koseki, Y. Aoyama, and K. Sako, "Simple modeling and prototype experiments for a new high-thrust, low-speed permanent magnet disk motor," in *Proc. Int. Conf. Electr. Mach. Syst.*, Nov. 2009, pp. 1–6.
[315] H. Weiss, "Drive with transversal flux machine," EP Patent EP1 239 571 (A1), Sep. 11, 2002.

BENEDIKT KAISER was born in Rottweil, Germany, in 1995. He graduated from High School in Villingen-Schwenningen and studied B.Eng. degree in mechanical engineering from the Cooperative State University of Mannheim. After gaining a year of industrial experience in research and development of ebm-papst, he began his M.Sc. degree in electromobility from the University of Stuttgart, in 2020. Since 2020, he has been with the Institute of Electrical Energy Conversion, University of Stuttgart. His research interests include novel actuators for application in robotics and transverse flux machines.

NEJILA PARSPOUR received the master's degree in electrical engineering and the Ph.D. degree *(summa cum laude)* from the Technical University of Berlin, in 1991 and 1995, respectively. She gained five years of industrial experience at Philips and six years of scientific experience at the University of Bremen. She is currently a Professor of electrical energy conversion at the University of Stuttgart and the Head of the Institute of Electrical Energy Conversion. Her research interests and teaching activities include electrical machines and drives with a focus on machine design and contactless energy transfer with a focus on inductive charging systems.